



UNIVERSITÀ POLITECNICA DELLE MARCHE
DIPARTIMENTO SCIENZE DELLA VITA E DELL'AMBIENTE

Corso di Laurea Magistrale
Biologia Marina

Tossicità di una miscela di nanoplastiche (NPs) e microplastiche (MPs) sul bivalve marino *Ruditapes decussatus*: confronto tra la tossicità della miscela rispetto a NPs e MPs considerate individualmente.

Toxicity of a mixture of NPs and MPs in *Ruditapes decussatus*: are mixtures less toxic than individual NPs and MPs contamination?

Tesi di Laurea Magistrale
di:

Eccezia Ventura

Relatore
Chiar.mo Prof.

Correlatore: (se previsto)

Maria João Beirão

Sessione 18 Luglio 2023

Anno Accademico 2022/2023

Toxicity of a mixture of NPs and MPs in *Ruditapes decussatus*: are mixtures less toxic than individual NPs and MPs contamination?

Emma Ventura

Masters in Marine Biology

Università Politecnica delle Marche

Centre for Marine and Environmental Research (CIMA) – University of Algarve
(Portugal)

Master Thesis

2022/2023

Supervisores: Prof. Doctor Francesco Regoli & Prof. Doctor Maria João Bebianno

Co-supervisor: Joanna M. Gonçalves



UNIVERSITÀ
POLITECNICA
DELLE MARCHE



INDEX

LIST OF FIGURES.....	1
LIST OF TABLES.....	1,2
LIST OF ACRONYMS AND ABBREVIATIONS.....	2,3
ABSTRACT.....	4
RIASSUNTO.....	5,6
1-INTRODUCTION.....	6-11
2-MATERIALS AND METHODS.....	11
2.1 Nano and microplastic particles.....	11,12
2.1.1 nPS and mPE characterization.....	12
2.2 Experimental design.....	13
2.2.1 Clams collection and acclimatization period.....	13,14
2.2.2 Experimental design.....	14
2.3 Sampling and tissue processing.....	14
2.3.1 Homogenization for enzymatic activity.....	15
2.3.2 Homogenization for Acetylcholinesterase (AChE) Activity.....	15
2.3.3 Homogenization for lipid peroxidation (LPO) evaluation.....	15,16
2.3.4 Homogenization for nPS ingestion.....	16
2.4 Ingestion.....	16,17
2.5 <i>In vitro</i> assay.....	17,18
2.6 Condition Index and mortality rate.....	18
2.7 Genotoxicity Assay (Comet Assay).....	18-20
2.8 Total protein evaluation.....	20
2.9 Acetylcholinesterase (AChE) activity.....	20,21
2.10 Enzymatic activity.....	21
2.10.1 Superoxide dismutase (SOD).....	21
2.10.2 Catalase (CAT).....	21,22
2.11 Lipid peroxidation.....	22
2.12 Quality control and assessment.....	22
2.13 Statistical analyses.....	22,23
2.14 Synergism and antagonism model.....	23
2.15 Weight of Evidence (WOE).....	23,24
3-RESULTS.....	24
3.1 nPS and mPE characterization.....	24,25

3.2 Ingestion.....	26,27
3.3 <i>In vitro</i> assay.....	27
3.4 Condition index and mortality rate.....	28
3.5 Genotoxicity Assay (Comet assay).....	28,29
3.6 Neurotoxicity assay (Acetylcholinesterase (AChE) activity).....	29-30
3.7 Enzymatic activities.....	30
3.7.1 Superoxide dismutase (SOD).....	30,31
3.7.2 Catalase (CAT).....	31,32
3.8 Lipid peroxidation.....	32,33
3.9 Principal Component Analyses PCA.....	33-34
3.10 Synergism and antagonism.....	35
3.10.1 Dose addition results.....	35,36
3.10.2.....	36,37
3.11 Weight of Evidence.....	37
4-DISCUSSION.....	37-44
CONCLUSION.....	44,45
BIBLIOGRAPHY.....	46-55

I would like to thank my supervisors,
professor Maria João Bebianno and professor Francesco Regoli,
for guiding me through this path.

I would also like to deeply thank my co-supervisor, Joanna Gonçalves,
for supporting me this entire time.

A special thank you goes also to all the researches of the ecotoxicological departments of
Universidade do Algarve and Università Politecnica delle Marche
for their fundamental help.

LIST OF FIGURES

Materials and Methods

Figure 2.1.1: Malvern MASTERSIZER 3000 (A); submergible stirrer (B).....	12
Figure 2.7.1: suspension of cells in LMA.....	19
Figure 2.7.2: slides in the electrophoresis chamber.....	19

Results

Figure 3.1.1: Hydrodynamic diameter of polystyrene nanoplastics (50nm) in ultrapure water.....	24
Figure 3.1.2: Average PSD obtained from laser diffraction analyses on nPS (50 nm) in a mixture with mPE (4-6 μm).....	25
Figure 3.1.3: PSD results from laser diffraction analyses on mPE (4-6 μm).....	25
Figure 3.1.4: Average PSD obtained from laser diffraction analyses on mPE (4-6 μm) in a mixture with nPS (50nm).....	26
Figure 3.2.1: amount of nanoplastics detected in the gills of clams expressed as μg of nanoplastic/ μg of wet tissue (A); amount of nanoplastics detected in the digestive gland of clams and expressed as μg of nanoplastic/ μg of wet tissue (B).....	26
Figure 3.2.2: mPE ingestion in gills of unexposed (CT), mPE and Mix exposed <i>R. decussatus</i> after 10 days (A); mPE ingestion in digestive glands of unexposed (CT), mPE and Mix exposed <i>R. decussatus</i> after 10 days (B).....	27
Figure 3.3.1: Differences in cell viability (Neutral Red dye) between <i>Ruditapes decussatus</i> unexposed hemocytes (CT), 24 h mPE (10 $\mu\text{g/L}$) exposed hemocytes, 24 h nPS (10 $\mu\text{g/L}$) exposed hemocytes, and 24 h Mix (10 $\mu\text{g/L}$ mPE + 10 $\mu\text{g/L}$ nPS) exposed hemocytes.....	28
Figure 3.5.1: Variation in the level of DNA damage (mean \pm sd) between different treatments (CT, mPE, nPS, Mix) and different days of exposure (0 and 7) in <i>Ruditapes decussatus</i> (A); Examples of comets in hemocytes of clams from all treatments (B).....	29
Figure 3.6.1: AChE enzymatic activity in gills of <i>Ruditapes decussatus</i> at different times of exposures (0, 7, and 10) and between different treatments (CT, mPE, nPS, and Mix).....	30
Figure 3.7.1: SOD activity changes in the gills (A) and digestive gland (B) of <i>Ruditapes decussatus</i> between different treatments (CT, mPE, nPS, Mix) and different times of exposure (0, 7, and 10).....	31
Figure 3.7.2: Catalase activity changes in gills (A) and digestive glands (B) of <i>Ruditapes decussatus</i> between different treatments (CT, mPE, nPS, Mix) and different times of exposure (0, 7, and 10)	32
Figure 3.8.1: LPO levels changes in gills (A) and digestive glands (B) of clams from different treatments (CT, mPE, nPS and Mix) and different days of exposure (0, 7, and 10).....	33
Figure 3.9.1: Principal component analysis (PCA) of a battery of biomarkers (CAT, SOD, LPO, AChE) in gills (A) and digestive glands (B) of <i>Ruditapes decussatus</i> for all treatments (CT, mPE, nPS, Mix) and all sampling days (0, 7, 10).....	34-35
Figure 3.11.1: Weight of Evidence (WOE) in relation to nPS, mPE, and Mix treatments and sampling days 7 and 10.....	37

LIST OF TABLES

Materials and Methods

Table 1: Description of the toxic algae that caused the bloom (IPMA, Resultados das Determinações de Fitoplâncton Nocivo, maio 2022; available at https://www.ipma.pt/pt/bivalves/biotox/docs/a-lbm-mai22.pdf)	13-14
---	-------

Table 2: Mortality rate during the experimental exposure.....	18
---	----

Results

Table 3: Dose addition results for the synergistic and antagonistic interactions between mPE and nPS in gills (SOD, CAT, LPO, neurotoxicity) and hemolymph (genotoxicity) of <i>Ruditapes decussatus</i>	35
--	----

Table 4: Dose addition results for the synergistic and antagonistic interactions between mPE and nPS in digestive glands (SOD, CAT, LPO) of <i>Ruditapes decussatus</i>	36
---	----

Table 5: Independent action results for the synergistic and antagonistic interactions between mPE and nPS in gills (SOD, CAT, LPO, neurotoxicity) and hemolymph (genotoxicity) of <i>Ruditapes decussatus</i>	36
---	----

Table 6: Independent action results for the synergistic and antagonistic interactions between mPE and nPS in digestive glands (SOD, CAT, LPO) of <i>Ruditapes decussatus</i>	37
--	----

LIST OF ACRONYMS AND ABBREVIATIONS

ACh	Acetylcholine
AChE	Acetylcholinesterase
ACT	Acetylcholine solution
BHT	Butylated hydroxytoluene
CAT	Catalase
CE	Capture efficiency
CI	Condition index
CT	Control
DAPI	6-diamidino-2-phenylindole
DCVJ	Molecular rotor probe 9-(dicyanovinyl)-julolidine
DG	Digestive gland
DMEM	Dulbecco's Modified Eagle Medium
DTNB	5,5'-ditio-bis (2-nitrobenzoato)
DTT	Dithiothreitol
EDTA	Ethylenediaminetetraacetic acid
FSW	Filtered seawater
GPP	Global plastic production
H ₂ O ₂	Hydrogen peroxide
HCl	Chloridric acid
HNE	4-Hydroxynonenal
K ₂ HPO ₄	Dipotassium phosphate
KCl	Potassium chloride

KH ₂ PO ₄	Potassium dihydrogen phosphate
LMA	Low melting point agarose
LOE	Line of Evidence
LPO	Lipid peroxidation
MDA	Malondialdehyde
Mix	Mixture of Polyethylene microplastics and Polystyrene nanoplastics
mPE	Polyethylene microplastics
MPs	Microplastics
Mt	Million tons
NaCl	Sodium Chloride
NaOH	Sodium hydroxide
NMA	Normal melting point agarose
NPs	Nanoplastics
nPS	Polystyrene nanoplastics
NR	Neutral Red
PCA	Principal component analyses
PE	Polyethylene
PP	Polypropylene
PS	Polystyrene
PSD	Particle size distribution
PVC	Polyvinyl chloride
ROS	Reactive oxygen species
S	Salinity
SDG	Sustainable development goal
SOD	Superoxide dismutase
T	Temperature
TP	Total protein
v/v	volume/volume
w.w.	wet tissue weight
WOE	Weight of evidence

ABSTRACT

The increased level of the micro (MPs) and nano-sized (NPs) plastic particles and the high levels of toxicity associated once these enter the ocean are highly concerning for the marine ecosystem. However, information relative to possible MPs/NPs interactions in the marine environment and the resulting possible changes in toxicity and ingestion pathways in marine biota are still to be understood. In this study, to assess the effects of MPs and NPs interaction, an *in vitro* (24 h) and an *in vivo* (10 d) exposure assay to polystyrene nanoparticles (nPS; 50nm, 10 µg/L), polyethylene microparticles (mPE; 4-6µm, 10 µg/L) and a mixture of the two (Mix; 10µg/L of mPE +10µg/L of nPS) were performed using the clam *Ruditapes decussatus*. A multi-biomarker approach was used to assess changes in genotoxicity, neurotoxicity, oxidative stress, damage, and the ingestion of MPs/NPs in clams' gills and digestive glands. For the *in vitro* exposure, the neutral red assay was used to assess cell viability in hemocytes of *R. decussatus* exposed to the three treatments (nPS, mPE, and Mix). Characterization of the MPs/NPs alone and as a mixture was also carried out. Bigger aggregates, meaning a higher level of aggregation, were formed concerning both mPE and nPS when in a mixture compared to when considered individually.

Ingestion was high for all treatments (mPE, nPS, and Mix) and tissues (gills and digestive gland), meaning that size is probably not the only selective mechanism used by *R. decussatus* to discriminate between particles. According to *in vitro* results, nPS is more toxic than mPE and Mix clam hemolymph. The increase in neutral red retention suggests an nPS localized toxicity on lysosomes of clam's hemocytes. With the *in vivo* results, no genotoxicity is reported. At the same time, an increase in AChE activity is observed in clams' gills after 7 days of exposure to mPE and 10 days of exposure to Mix. mPE, nPS, and Mix treatments caused a critical increase ($p<0.05$) in CAT and SOD activity in gills and digestive glands, meaning that the exposure to contaminants caused a higher ROS production. Antioxidant enzyme (SOD, CAT) activity changes are time and tissue related. Day 10 is the most influential day on the overall hazard, and the digestive gland is the most impacted tissue. Furthermore, mPE and Mix are the most influential treatments on the overall biomarker responses. Nonetheless, no signs of lipid peroxidation were detected in both tissues (gills and DG), meaning that the antioxidant defense system could counteract the generation of ROS by the plastic particles, individually and as a mixture. nPS, due to their small size, appear to cause the highest toxicity at the cellular level. An antagonistic interaction may occur between the two sizes of plastic particles.

Keywords: Microplastics, nanoplastics, Ruditapes decussatus, biomarker.

RIASSUNTO

L'aumento nel numero di micro (MPs) e nano (NPs) frammenti di plastica insieme al loro elevato livello di tossicità una volta raggiunto il mare sta diventando un problema di grande importanza per l'intero ecosistema marino. Tuttavia ad oggi non ci sono ancora informazioni su come la possibile interazione tra MPs e NPs possa influenzare la loro tossicità e ingestione da parte della fauna marina. In questo studio la vongola verace *Ruditapes decussatus* è stata esposta, utilizzando protocolli *in vitro* (24h) e *in vivo* (10 giorni), a microplastiche di polietilene (mPE), nanoplastiche di polistirene (nPS) e a una miscela delle due (Mix), per comprendere possibili cambiamenti nel livello di tossicità delle plastiche quando sono presenti contemporaneamente in acqua. A questo scopo, diversi biomarker di genotossicità, neurotossicità, stress e danno ossidativo, insieme all'identificazione del livello di ingestione di MPs e NPs, sono stati analizzati sia a livello delle branchie che a livello della ghiandola digestiva delle vongole. Il test del "Rosso Neutro" è stato utilizzato per individuare i livelli di vitalità cellulare degli emociti di *R. decussatus* esposti *in vitro* ai tre diversi trattamenti (nPS, mPE e Mix). Inoltre, è stata eseguita una caratterizzazione in termini dimensionali delle NPs e MPs quando sospese individualmente e quando in miscela. Si osserva una maggiore tendenza all'aggregazione con formazione di aggregati di maggiori dimensioni per le plastiche in miscela rispetto a quelle sospese in acqua individualmente. Il livello di ingestione di MPs e NPs è elevato per tutti i trattamenti (nPS, mPE e Mix) e i tessuti analizzati (branchie e ghiandole digestive) indicando probabilmente che la dimensione dei frammenti di plastica non è l'unico meccanismo di selezione utilizzato dalla *R. decussatus* per discriminare il materiale che può essere ingerito. I risultati ottenuti dall'esposizione *in vitro* indicano come le vescicole lisosomiali degli emociti di *R. decussatus* sono maggiormente danneggiati dall'esposizione alle nPS rispetto agli altri trattamenti, mentre quelli ottenuti dall'esposizione *in vivo* mostrano l'assenza di genotossicità e neurotossicità con un aumento però dell'attività enzimatica dell'acetilcolinesterasi (AChE) nelle branchie di *R. decussatus* esposte per 7 giorni alle mPE e per 10 giorni alla Mix ($p < 0.05$). È stato anche osservato un aumento di attività per gli enzimi catalasi (CAT) e superossido dismutasi (SOD) in relazione a tutti i trattamenti (nPS, mPE e Mix) e i tessuti analizzati (branchie e ghiandole digestive) probabilmente a causa di un aumento nella produzione di specie reattive dell'ossigeno (ROS) in seguito all'esposizione ai contaminanti. Cambiamenti dell'attività enzimatica risultano inoltre essere più evidenti al giorno 10 (fine dell'esposizione) e nella ghiandola digestiva. I trattamenti mPE e Mix sono quelli che più influiscono sui cambiamenti complessivi dei biomarker considerati. Nonostante ciò, non risulta un aumento di perossidazione lipidica (LPO) in nessuno dei due tessuti esposti, suggerendo che il sistema antiossidante dell'organismo sia in grado di neutralizzare la formazione di ROS. Le nPS a causa della

loro ridotta dimensione risultano avere una maggiore tossicità a livello cellulare. È quindi possibile suggerire l'insorgenza di interazioni antagonistiche tra NPs e MPs quando presenti in miscela.

Parole chiave: microplastiche, nanoplastiche, Ruditapes decussatus, biomarker.

1-INTRODUCTION

Plastics are a unique set of materials that have changed our way of living since the beginning of their production in the late 19th century. Lightweight, durability, and low cost of production are only a few of the most important properties that make plastics the most used type of synthetic material worldwide. The final synthetic plastic macromolecule is a polymeric chain, a group of several monomers bonded together through a polymerization or polycondensation chemical reaction. Monomers are single molecules with different characteristics and properties that can form different polymeric chains based on their molecular structure. The high level of versatility that characterize polymerization and polycondensation reactions, and the possibility of binding together different monomers with unique properties, allow the production of always new, innovative, and more efficient plastic materials. Plastic can be applied in almost every sector: agriculture, automotive, domestic use, the textile industry, transportation, building & construction, production of packaging for the food industry, etc. As a result of the high applicability of plastic materials, they became, since their commercial development between 1930 and 1940, an essential component of the world's economy, improving the quality of life for millions of people around the globe. Therefore, global plastic production (GPP) increased exponentially, reaching 288 million tons in 2012, 365.5 Mt in 2018, and 390.7 million tons in 2022 (PlasticsEurope, 2022; Van Cauwenberghe et al., 2015). More so, predictions show GPP to increase even more, potentially reaching around 600 million tons by 2025 and exceeding one billion tons by 2050 (FAO - Microplastic in Fisheries, 2017).

Considering only European countries, the European plastic industry provides one of the highest levels of employment and contribution to the European fabric industry, supporting the development of the entire European economy (PlasticsEurope, 2022). After a slight decrease in European plastic production (53.9 Mt in 2020) due to the COVID-19 pandemic, in 2021, an increasing trend of 4% with a total production of 57.2 Mt (15-19% of GPP) was observed (PlasticsEurope, 2022).

Polyethylene (PE), polypropylene (PP), polyvinyl chloride (PVC), and polystyrene (PS) are among the most requested polymers by the global plastic industry with, therefore, a high percentage of production (26.9% PE, 19.3% PP, 12.9% PVC and 5.3% PS) (PlasticsEurope, 2022). Especially PE and PS are highly used in packaging (e.g., coffee cups, takeaway lids, detergents bottles, milk

cartoons) and building & construction (e.g., rigid pipes, park benches, air conditioners, roofing, building walls) end markets that indeed have the highest level of contribution to the GPP (44% and 18% respectively) (PlasticEurope, 2022). The presence of such polymers in the environment is concerning. PS is a high-density polymer whose accumulation is mostly detected in the marine benthic compartment. However, changes in its density due to different weathering phenomena can also cause its flotation and, therefore, its accumulation in the surface layer (Pirsaheb et al., 2020). PS's high frequency of accumulation in the gut of several marine organisms was documented (Pirsaheb et al., 2020), as well as its possible translocation in different tissues of aquatic species (Browne et al., 2008; Hsieh et al., 2023; Lei et al., 2018; Pirsaheb et al., 2020; Ziccardi et al., 2016). On the other hand, PE has low-density properties and so a major presence on the seawater surface with, also, in this case, possible detections in the benthic system due to changes in its density (Pirsaheb et al., 2020). PE, being a non-biodegradable polymer, can persist in the marine environment for a long-time causing harm to the marine biota (Baudrimont et al., 2020; El-Sherif et al., 2022; Lei et al., 2018; Pirsaheb et al., 2020; Ziccardi et al., 2016). Ter Halle et al. (2017) found high PE, PP, PVC, and PS percentages in samples collected in the North Atlantic subtropical gyre. Interestingly a wider variety of polymers with a reduction in size was found. PE (90%) and PP (10%) were the only ones found between mesoplastics and large microplastic fragments. In contrast, when analyzing smaller microplastics and nanoplastics, PVC (8%) and PS (2%) were also found (Ter Halle et al., 2017). This can be related to the higher level of persistence of the non-biodegradable PE polymer compared to other polymers like PS, which may be degraded more rapidly and accumulate as smaller fragments (Ter Halle et al., 2017; El-Sherif et al., 2022; Pirsaheb et al., 2020).

The current increasing trend in plastic production and the increasing human population density are strictly correlated to the growing number of plastic materials entering the ocean (Jambeck et al., 2015). Even though an increasing trend (+117%) in plastic recycling was observed from 2006 until today, there is still an important percentage (37%) of plastic waste that, due to the lack of appropriate waste management systems, ends up in landfills or reaches the marine environment (PlasticEurope, 2022; Alimi et al., 2018). Indeed, the primary sources of pollution are human-related and from either land (e.g., residential & domestic activities, tourism, recreational activities) or ocean-based activities (offshore fishing, aquaculture, and navigation activities) (Thushari & Senevirathna, 2020). This has a huge impact on the health status of the whole marine environment, giving rise to negative consequences towards marine biota, as well as repercussions on goods (e.g., food, pharmaceutical components, mineral sources) and services (e.g., climate regulation, carbon sequestration, oxygen production) that the ocean provides to our society. Adverse effects are aggravated by the increasing concentration of smaller plastic fragments (Kiran et al., 2022). Indeed, once plastic materials enter

the marine environment, they can undergo several degradation and fragmentation processes, such as UV-induced photodegradation, thermo-oxidation, hydrolysis, and microbial degradation, that eventually cause their size reduction, reaching a measurement scale between micro (μ) and nano (n) meters. Ekvall and colleagues (2019) demonstrated the formation of PS nanoplastic (nPS) fragments from coffee cups and takeaway lids by mimicking weathering processes occurring in seawater.

Still, despite the trim level of consensus reached among the scientific community, microplastics and nanoplastics are commonly defined as particles with a size range of 1 μ m to 5 mm and 1 nm to 1000 nm, respectively (Gigault et al., 2018; Guzzetti et al., 2018). Primary and secondary micro (MPs) and nanoplastics (NPs) can be distinguished in the marine environment based on their origin and how they enter this environment. Primary MPs and NPs particles are manmade to a specific size range and used in many applications and consumer products (e.g., personal care products, medical products, industrial abrasives, clothing fibers, ink for 3D printers) (Duis & Coors, 2016; Gonçalves & Bebianno, 2021). The excessive use of such products, along with their improper disposal and handling can lead to the entrance, directly or indirectly through wastewater treatment plants (WTTP), of high amounts of these tiny plastic particles into the ocean with their original small size (Duis & Coors, 2016); up to 10 million nano-sized plastic particles can be released into the environment by a single use-facial scrub (Kiran et al., 2022). Secondary micro- and nano-plastics, on the other hand, are produced by the fragmentation (e.g., weathering) of bigger plastic objects that have reached the marine environment (Duis & Coors, 2016).

These tiny plastic particles are particularly resistant to biodegradation, and they have the potential to remain in the environment for hundreds of years (Guzzetti et al., 2018). Therefore, since their first evidence in seawater in the 1970s (Carpenter and Smith, 1972), a high concentration of micro and nanosized plastics fragments has now reached many areas of the marine environment, such as intertidal ecosystems, deep-sea sediments, surface waters, and Polar regions (Guzzetti et al., 2018; Peeken et al., 2018). At least 5.25 trillion pieces of microplastic are thought to be floating in the ocean (Ter Halle et al., 2017). This issue was assessed by the United Nations Sustainable Development Goals (SDG 14- Life below water) (Kiran et al., 2022) and even though many studies have been conducted to better understand MPs/NPs sources, distribution, and toxicity pathways, many gaps, especially in relation to NPs, are still to be filled due to a lack of analytical methodologies to quantify and assess their effects (Baudrimont et al., 2020; Gonçalves & Bebianno, 2021; Hsieh et al., 2023; Zaki & Aris, 2022).

A reduction in the size of the plastic particles causes an augmentation of their biological reactivity resulting in higher toxicity (Gonçalves & Bebianno, 2021). The formation and the persistence of MPs and NPs fragments in water can alter their physical and chemical properties (Li et al., 2019; Zhang et

al., 2021). For instance, free ions present in seawater can be absorbed by MPs particles changing their surface charges (Rahman et al., 2023), thus allowing them to possibly form aggregates that influence their fate, mobility and reduce their bioavailability for marine organisms (Gonçalves & Bebianno, 2021; Li et al., 2019).

It is well known that plastics can act both as sinks and sources of many toxic compounds in the marine environment; indeed, plastic materials can either contain toxic additives deriving from the manufacturing process or can absorb contaminants dispersed in seawater and sediments (e.g., persistent organic pollutants, metals, and hydrophobic organic chemicals) (Alimi et al., 2018; Vital et al., 2021; Ziccardi et al., 2016). MPs and NPs, due to their smaller size, have a bigger surface area and so a higher capacity to absorb and release contaminants, either after ingestion or during their degradation process in seawater (Alkimin et al., 2022; Islam et al., 2021), posing a significant additional risk for the marine biota. However, the biggest concern with the presence of MPs and NPs in the marine environment is that their small size allows them to be easily ingested by many marine organisms (Rodrigues et al., 2022) either accidentally or because of their similitude to the prey (Fossi et al., 2018). The smaller the particles size, the easier it is for them to cross biological membranes, thus causing bioaccumulation and biomagnification along the trophic food web, all the way up to humans (Baudrimont et al., 2020; Gonçalves & Bebianno, 2021; Kiran et al., 2022). A high number of plastic particles were found in seafood (e.g., cultivated bivalves), and 0.5 g of plastic per week was calculated to be ingested in Europe due to contaminated seafood consumption (Vital et al., 2021; Kiran et al., 2022).

Furthermore, MPs and NPs' ability to cross biological membranes can also cause their penetration into cells and tissues (Capolupo et al., 2021), inducing mechanical and physical damage (e.g., blockage of feeding structures, inflammation, abrasion) along with the alteration of critical biological functions (e.g., genotoxicity, neurotoxicity damage) in many marine organisms (Fossi et al., 2018; Gonçalves et al., 2022; Guzzetti et al., 2018; Zaki & Aris, 2022).

Bacteria and algae are important constituents of the marine ecosystem contributing to its health, nutrient cycling, and oxygen production (Gonçalves & Bebianno, 2021). Alarmingly, the presence of MPs and NPs particles can negatively affect organisms with significant possible cascade effects on the ocean environment. Ning et al. (2022); Sun et al. (2018); Ustabasi & Baysal, (2020) assessed the presence of growth inhibition along with increased ROS production and oxidative damage in bacteria (*Bacillus subtilis*, *Escherichia coli*, *Pseudomonas aeruginosa*, *Staphylococcus aureus*, *Escherichia coli*, and *Halomonas alkaliphilia*) exposed either to PE or PS MPs/NPs particles. Furthermore, negative consequences to MPs and NPs exposure such as growth inhibition, reduction in photosynthetic capacity, loss of membrane integrity and decreasing levels in DNA content were

observed in *Rodoma baltica*, *Tetraselmis chuii*, *Nannochloropsis gadittana*, *Isocrysis galbana* and *Thalassiosira weissflogii* (Gomes et al., 2020; Venâncio et al., 2019). Primary, secondary, and tertiary consumers, such as many invertebrates and fish species, were also negatively affected by the presence of smaller plastic fragments (Barboza et al., 2018; Bergami et al., 2019; Brandts et al., 2018, 2021; Espinosa et al., 2018; Gambardella et al., 2017; Horn et al., 2020; Lee et al., 2013; Mohsen et al., 2021; Wang et al., 2021). In 2017 Manfra et al. studied the increasing mortality in rotifers (*Brakionus koreanus*, *Brachionus plicatilis*) exposed for 24h and 48h to different sizes of NPs, while Wang et al., in 2019, found oxidative stress, histological effects, and negative consequences on the reproduction of the fish *Oryzias melastigma* when exposed to 10 µm PS MPs.

Marine bivalves, due to many characteristics (e.g., worldwide distribution, high filtering capacity, interaction with both sediments and seawater, high bioaccumulation capacity, ability to filter and capture small particles), are important sentinel organisms that can therefore be used to better understand the effects possibly caused by contaminants present in the marine environment (e.g., plastic particles) (Bebianno et al., 2004; Sendra et al., 2021; Silva et al., 2021). It has been already demonstrated the capacity of marine bivalves to ingest plastic particles of small size that can then be translocated and accumulated in many tissues (e.g., gills and digestive gland) (Bendell et al., 2020; Ribeiro et al., 2017; Magara et al., 2018; Sendra et al., 2021; Thomas et al., 2020). Genotoxicity, neurotoxicity, oxidative stress, and oxidative damage have also been assessed in filter-feeding organisms such as mussels (*Mytilus galloprovincialis*, *Mytilus coruscus*, *Mytilus edulis*) and clams (*Scrobicularia plana*, *Ruditapes decussatus*) (Bebianno et al., 2004; de Alkimin et al., 2022; Huang et al., 2021; Islam et al., 2021), with increasing effects concerning smaller particles sizes (Capolupo et al., 2021).

The clam *Ruditapes decussatus* is a suitable biological indicator that allows to obtain important evaluations of environmental pollution gradients due to its high filtering capacity and wide distribution (Anhichem et al., 2021; Bebianno et al., 2004). Furthermore, its high protein and fatty acids content make *R. decussatus* an important source for human consumption in many countries (Bebianno et al., 2004). For example, in the Ria Formosa lagoon, south coast of Portugal, the rearing of the specie represents one of the most important economic activities producing 80% of the consumed shellfish in Portugal and occupying about 395 ha of the entire intertidal area (Bebianno et al., 2004; Cozzolino et al., 2021; Duarte et al., 2020). However, the increasing levels of contaminants polluting the environment and bivalves' capacity to accumulate anthropogenic compounds make this species unsuitable for human consumption (Anhichem et al., 2021; Bebianno et al., 2004). In the Ria Formosa lagoon, an important problem of water deterioration is present due to a constant input of many pollutants (e.g., fertilizers, high amounts of organic matter, pesticides, and personal care

products) deriving from different human activities in and around the lagoon itself (Aníbal et al., n.d.; Cozzolino et al., 2021). Even though an implementation in management strategies were recently carried out in the area, high concentrations of these contaminants are still detected in the lagoon's water with important consequences not only for the marine biota but also in relation to human health (Aníbal et al., n.d.; Cozzolino et al., 2021).

As part of the RESPONSE project (JPI Oceans), this study contributes to increase our knowledge of the fate and biological effects of both nano and microplastic particles. In this particular case, the objective is to evaluate how MPs and NPs of two highly produced plastic polymers, PE and PS, respectively, interact in the water medium and how this can influence the physiological effects on *R. decussatus* also considering that a possible aggregation of the plastic particles can increase their size, therefore, decreasing the probability of ingestion and translocation by filter-feeding organisms. MPs and NPs characterization analyses (hydrophobic diameter, particle size distribution) were conducted to understand plastics behavior in a water medium.

Ruditapes decussatus organisms were submitted to a 10-day exposure to evaluate the effects of 10 µg/l polyethylene MPs (mPE) (4-6 µm), 10 µg/l polystyrene NPs (nPS) (50 nm), and 20 (10+10) µg/l of a mixture of the two (Mix). A multi-biomarker approach was used to evaluate oxidative stress (SOD, CAT), oxidative damage (LPO), genotoxicity, neurotoxicity (AChE), and ingestion of micro and nanoplastics. Furthermore, an *in vitro* assay (24 h) was carried out to evaluate the level of cell viability in the hemolymph of exposed clams (mPE, nPS, and Mix). The results of biomarkers analyses were analyzed for synergistic and antagonistic effects and finally integrated using the Weight of Evidence (WOE) quantitative model.

2-MATERIALS AND METHODS

2.1 Nano and microplastic particles

Two different types of plastic particles were used: fluorescent virgin Polystyrene (PS) Nanoplastics (NPs) of 50 nm in size and virgin Polyethylene (PE) Microplastics (MPs) of 4-6 µm in size. Fluoresbrite® Plain YG 0.05 µm Microspheres (9003-53-6) were purchased from Polysciences, Inc. (Germany). 0.05 µm PS nanoparticles (nPS) packed as 2.5% aqueous suspension, 3.64×10^{14} particles/mL in water (7732-18-5), CV=15%, excitation max.=441nm, emission max.=486nm. PE MPs (mPE) (MPP-635XF; density: 0.96) were purchased from Micro Powders Inc. (NY-USA). A 10mg/L stock solution of mPE particles was made for the experiment by mixing 10 mg of mPE

particles with 1L of distilled water. After being prepared the solution was placed on the magnetic stirrer for 30 min and then sonicated overnight to prevent particles from floating at the surface.

2.1.1 nPS and mPE characterization

A DLS particle sizer (ZetaSizer Nano ZS90, Malvern Inc.) was used to determine the hydrodynamic diameter of nPS in both ultrapure water [7732185] and filtered seawater (FSW). The same instrument was used to evaluate zeta potential values of nanoplastics through electrophoresis mobility measurements performed at 25°C in a 1x1x1 disposable polycarbonate capillary cell. Aggregation kinetics were assessed between 2- and 12 hours using time-resolved DLS measurements. A gap of 50s was estimated between the start of aggregation and data collection.

According to Ramaswamy & Rao (2006), a precise and fast technique to define particles size distribution (PSD) is the laser diffraction method that was applied in this study to define the behavior, in aqueous solution, of individual mPE particles and of a mixture of nPS and mPE. This methodology is based on the principle that a particle of a certain size diffracts light at a certain angle, the latter decreases as the particle size increases (Ramaswamy & Rao, 2006; Rodríguez & Uriarte, 2009). Specific detectors measure the scattered light angle, allowing us to obtain data on the PSD (Ramaswamy & Rao, 2006).

For the analyses, the Malvern MATERSIZER 3000 was used (Figure 2.1.1 A). Two plastic suspensions were made in separate 600 ml beakers. The first one was prepared by adding 0.1 g of mPE (4-6 µm) particles in 500 ml of ultrapure water, while the second one was by adding 0.1 g of mPE particles and 1 ml of the nPS (50 nm) aqueous solution in 500 ml of ultrapure water. For the mixture, the analyses were conducted twice, one selecting PE as the polymer to analyze and the other one selecting PS. Six consecutive measurements were carried out by the Malvern, and the particles were maintained suspended by a submersible stirrer (Figure 2.1.1 B). Before starting, the Malvern was calibrated using only ultrapure water.

Results are expressed both in terms of percentage volume (%volume) and particle size (µm).

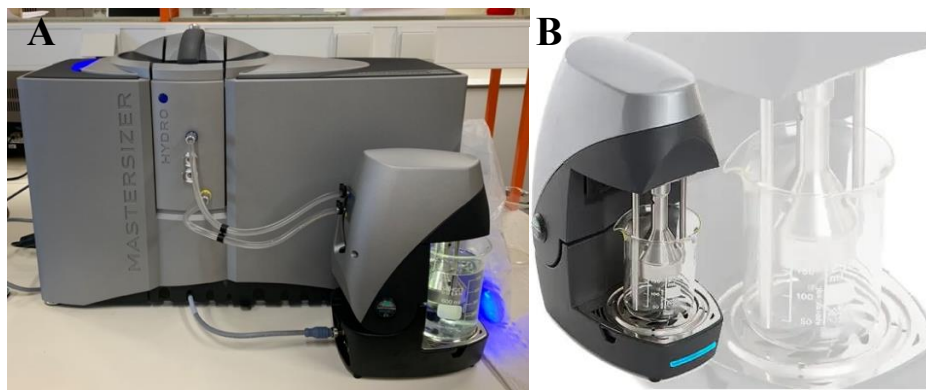


Figure 2.1.1: (A) Malvern MASTERSIZER 3000 (B) submersible stirrer

2.2 Experimental design

2.2.1 Clams collection and acclimatization period

The model organism for the experiment was the clam species *Ruditapes decussatus*. Specimens were purchased from Formosa-Cooperativa de Viveiristas da Ria Formosa, an aquaculture facility situated in Porto de Pesca de Olhão Apartado 1002, Olhão, Portugal, 8700-282450 (37.007117-7.834466).

Before the arrival of the organisms, 9 glass aquariums of 30 L capacity were prepared for the acclimatization period. Each tank was sterilized using a 10% HCl solution and deeply washed with distilled water. Following, filtered (0.45 µm) natural seawater (S:35± 3 psu; T:21.3±0.18 °C; pH:7.91±0.05) from the Ria Formosa lagoon, Faro, Portugal, was used to fill each aquarium up to 20L. This was used throughout the entire experiment.

Once clams arrived at the laboratory, they were divided into each one of the 9 tanks previously prepared (2.5 clams/L) and acclimatized for 7 days under constant aeration and a 12 h/12 h light/dark cycle. During these 7 days, clams were fed only with the plankton found in natural seawater.

Each aquarium was checked every day to remove potential dead organisms that could affect the other individuals in the tank. Every other day each aquarium was emptied and filled again with 20L of fresh filtered natural seawater.

There has been an exceptionally high level of mortality during the acclimatization due to a bloom of different toxic algae species in the Ria Formosa lagoon (Table 1); this contaminated the filtered seawater used to fill the aquariums. For this reason, to ensure that the experiment would not be compromised by the physiological status of organisms, the condition index was evaluated in 5 clams randomly selected from various tanks at the end of acclimatization.

Table 1: Description of the toxic algae that caused the bloom (IPMA, Resultados das Determinações de Fitoplâncton Nocivo, maio 2022; available at <https://www.ipma.pt/pt/bivalves/biotox/docs/a-lbm-mai22.pdf>)

Date	Group of marine algae	Type of toxin produced
9/05/2022	1) Bacillariophyceae	1) domoic acid
11/05/2022	1) Bacillariophyceae	1) domoic acid
	2) Dinophyceae	2) Okadaic acid, dynophisistoxins and pectenotoxins
	3) Dinophyceae	3) Azaspiracid
	4) Dinophyceae, Raphidophyceae and Haptophyta	4) Toxic at elevated biomass
17/05/2022	1) Bacillariophyceae	1) domoic acid
	2) Dinophyceae	2) Okadaic acid, dynophisistoxins and pectenotoxins
	3) Dinophyceae	3) Yessotoxin and Homoissotoxin
	4) Dinophyceae	4) Azaspiracid

25/05/2022	1) Dinophyceae	1) Azaspiracid
30/05/2022	1) Dinophyceae	1) Okadaic acid, dynophisistoxins and pectenotoxins

2.2.2 Experimental design

Individuals of *R. decussatus* were exposed in duplicates for 10 days to four different treatments: 1) control (CT); 2) 10 µg/L of mPE particles (mPE); 3) 10 µg/L of nPS particles (nPS); and 4) 10µg/L mPE +10µg/L nPS (Mix). At day 0, 7 and 10, organisms were randomly collected from each tank to conduct further analyses on a battery of biomarkers of oxidative stress and damage, neurotoxicity, genotoxicity along with the ingestion of plastic particles.

At the end of the 7 days acclimatation and after the collection of 34 animals for day 0 analyses, the aquariums were prepared for the experimental exposure; each one of the 8 tanks (duplicate design, two aquariums per treatment) were filled with 13 L of filtered sea water (S:35± 3 psu; T:21.3±0.18 °C; pH:7.91±0.05) and 39 animals per aquarium were added. The volume of water was calculated to have a ratio of 2.5 clams/L. After each sampling day, the water volume was adjusted to the number of clams in each tank, and the amount of plastic solution to add to obtain the final target concentration of 10 µg/L was calculated based on the volume of water added.

During the experiment clams were fed only with the plankton contained in natural seawater and were maintained under constant aeration and a 12 h/12 h light/dark cycle.

The aquariums were monitored every day to assess mortality and remove possible dead animals.

The seawater was changed every other day and nPS and mPE stock solutions were added after every water exchange.

Salinity, temperature, pH, and the level of O₂ saturation were measured every other day prior changing the water using a multiparametric probe (ODEON V3.3.0); the abiotic parameters remained stable during the entire duration of the experiment (S: 37.8±2.2; T:19.0±0.8 °C; pH:7.8±0.1; O₂ saturation: 100 ±1.7%).

2.3 Sampling and tissue processing

Clam specimens were randomly collected from each aquarium on days 0, 7, and 10. Immediately after collection, the hemolymph was extracted from clams' abductor muscles using a sterile hypodermic syringe (1 mL; 25 G needle), and genotoxicity analyses on hemocytes were conducted on the same day. Animals were then dissected, and each organism's gills and digestive glands were instantly frozen at -80°C until further analyses. Only on day 0 (section 2.2.1) five organisms were dissected, and the whole tissue weight, both wet and dry, was measured to calculate the CI.

For analyses, tissues were processed following specific protocols.

2.3.1 Homogenization for enzymatic activity

Gills and digestive glands from each treatment and each sampling day (0, 7, and 10) previously flash frozen (-80°C) were slowly defrosted on ice, transferred in decontaminated and properly labeled falcons, and weighed. Each tissue was then individually homogenized by adding 5 ml of Tris-Sucrose buffer (0.5 M Sucrose, 0.075 M KCl, 1 mM DTT, 1 mM EDTA, pH 7.6) in each falcon and then by mixing with a star-beater (VWR). Then, homogenized tissues were centrifuged twice to isolate the cytosolic fraction in the supernatant, first at 500 g and 4°C for 15 mins, followed by 12 000 g and 4°C for 40 min.

The supernatant of each sample was then collected and divided into 4 aliquots in properly labeled Eppendorf tubes:

- one for total protein analyses
- one for CAT activity analyses
- one for SOD activity analyses
- one for G6PDH activity analyses

Samples were immediately frozen at -80°C to guarantee their preservation.

2.3.2 Homogenization for Acetylcholinesterase (AChE) Activity

Gills previously flash frozen at -80°C were slowly defrosted on ice, transferred singularly to decontaminated and properly labeled falcons, and weighed. Individual tissue was then homogenized with 3ml of buffer (100 mM Tris-HCl solution (pH 8) and 30 µl of Triton solution 0.1%) added to each falcon; the latter was then mixed using a star-beater (VWR). Once homogenized, samples were centrifuged at 12 000 g and 4°C for 30 minutes to isolate the cytosolic fraction contained in the supernatant.

After homogenization, the supernatant of each sample was divided into two aliquots and transferred in two properly labeled Eppendorf's: one for total protein (TP) evaluation and the other one to conduct AChE activity analyses. Eppendorf tubes were immediately frozen at -80°C.

2.3.3 Homogenization for lipid peroxidation (LPO) evaluation

Gills and digestive glands previously frozen (-80°C) were slowly defrosted on ice, weighed, and transferred to 15 ml falcons. Each tissue was then individually homogenized with the star-beater (VWR) after adding, to each falcon, 5 ml of 0.02 M Tris-HCl buffer and 50 µl (1µl for each ml of Tris-HCl) of butylated hydroxytoluene (BHT) solution.

After homogenization, samples were centrifuged at 30 000g and 4°C for 45 mins. Subsequently, after centrifugation, the supernatant of each sample containing the cytosolic fraction was divided into two aliquots, one for the total protein evaluation and one for the LPO assessment; Eppendorf tubes were then immediately frozen at -80°C.

2.3.4 Homogenization for nPS ingestion

Gills and digestive glands previously frozen (-80 °C) from each treatment and from each sampling day (0 and 10) were slowly defrosted on ice and weighed. Samples were then transferred in properly labeled falcons and added 2 ml of ice-cold homogenization buffer solution (50 mM NaCl, 10 mM Hepes-NaOH (pH 7.4), 1 mM EDTA, 1 mM DTT). A star-beater (VWR) was used to homogenize the samples (5 min, 20/s shaking, with grinding balls). Homogenates were then centrifuged for 20 minutes (2 °C, 15 000 g) to isolate the cytosolic fraction; the supernatant was divided into two aliquots (ingestion and TP), transferred in properly labeled Eppendorf tubes and immediately frozen (-80°C) until further analyses.

2.4 Ingestion

nPS and mPE particle ingestion was evaluated in both gills and digestive glands. Six clams collected from CT, mPE, or nPS and Mix treatments were dissected into gills and digestive glands and weighed and kept at -80°C until further analysis.

nPS particle ingestion was measured using the microplate spectrofluorometric method developed by (Gagné, 2019). This fluorescence-based methodology uses the properties of the commercially available molecular rotor probe 9-(dicyanovinyl)-julolidine (DCVJ) (purchased from Sigma Aldrich) to detect changes in hydrophobicity and microviscosity.

Previously homogenized gills and digestive glands from CT, nPS, and Mix treatments collected at days 0 and 10 were slowly defrosted on ice. In the meantime, the solid DCVJ probe was dissolved at a concentration of 1 mM in methanol and stored in the dark at 4°C. Just before analyses, the DCVJ probe was diluted at 10 µM in Milli-Q water. Samples were incubated with the DCVJ probe in the dark for 10 minutes using a dark-well microplate; subsequently, nPS detection was performed using a microplate fluorimeter (Tristar 5 Multimode Microplate Reader) that detected an emission spectrum between 480-800 nm at 450 nm excitation. A standard curve was obtained from a known concentration of nPS to calculate the nPS weight in the samples. nPS highest excitation was found at 510 nm. Results are expressed relative to control as µg of nPS/g of wet tissue.

mPE ingestion, on the other hand, was evaluated using the density separation method (Bebianno et al., 2022). At sampling day 10, six clams from CT, mPE, and Mix treatments were collected and subsequently dissected into gills and digestive glands. Six gills and digestive glands per treatment were weighed together and then digested over 2 days at 50°C using a 10% KOH (Potassium hydroxide) solution with a ratio of 5:1 ml per gram of tissue.

Pre-filtered NaCl (Sodium Chloride) solution with a density of 1.2 was added separately to each digested sample to allow plastic particles to float. After an incubation period of 30 minutes, the superficial layer of the solution was collected in a glass beaker and then filtered to collect mPE particles. A Vacuum pump (Pall®) and cellulose filters with a mesh size of 0.45 µm were used. Once dry, the filters were colored with Nile Red. A working solution of 5 µg/ml of the latter was prepared from a 1mg/ml stock solution. 2 ml of working solution was then added to the filters, which, once dried, were observed under a light microscope (Compound Light Microscopy; 400x) to measure the size of the mPEs. Pictures of the filters were taken using a camera (Moticam 1080), and the images were analyzed for plastic detection using the program Motic Image Plus 3.1.

2.5 In vitro assay

In vitro analyses were conducted following the adapted Gómez-Mendikute & Cajaraville (2003) and Katsumiti et al. (2014) protocols.

20 individuals of *Ruditapes decussatus* were purchased from Formosa-Cooperativa de Viveiristas da Ria Formosa (37.007117-7.834466). They were acclimatized for 4 days (12h/12h light/dark cycle) in a 10 L glass tank (2 clams/L) filled with filtered natural seawater. After acclimatization, hemolymph was extracted from the clams' abductor muscle using a sterile hypodermic syringe (1 mL; 25 G needle) under aseptic conditions in a vertical laminar airflow cabinet. In ice, 5 pools of 4 clams each were prepared for each treatment (CT, mPE, nPS and Mix). From each pool, 10µl of hemolymph were taken and placed in an anti-aggregation solution (0.2M Tris; 171 mM NaCl; 24 mM EDTA; 0.15% v/v HCl 1N) (Katsumiti et al., 2014) to avoid cell aggregation. Different Eppendorf tubes were used for each treatment.

Cell viability was then assessed firstly by staining 10 µl of hemolymph with 10 µl of Trypan Blue Stain (0.4%) and then by counting the percentage of alive cells in a group of 100 randomly counted cells according to the formula:

$$\text{Concentration (cells mL}^{-1}\text{)} = \frac{n^2 \text{ cells} \times 10\,000}{n^2 \text{ squares}} \times \text{dilution factor}$$

A Neubauer chamber, a hemocytometer, and light microscopy (Compound Light Microscopy; 400x) were used. Once this was calculated, a hemolymph volume containing 2x10⁵ cells/mL cell concentration was suspended in an anti-aggregation solution.

In 96-well microplates, 100 µl of hemolymph were placed in the cell culture media Dulbecco's Modified Eagle Medium (DMEM, pH 7.4) (6 replicates per treatment), and 10 µl of nPS (50 nm), 10 µl of mPE (4-6µm) and 10+10 µl of nPS and mPE were added respectively for nPS, mPE and Mix treatments. In controls, no plastic was added. Microplates were then incubated for 24 hours at 18°C. Once ready, the DMEM medium was removed from the microplate wells, and cell status was checked using light microscopy (Compound Light Microscopy; 400x). Neutral red working solution (0.4%, pH 7.3-7.4) was added to each well plus 6 empty ones for negative controls and then incubated for 1 hour in the dark. Microplates were then centrifuged at 4°C for 10 minutes to separate the supernatant. The latter was then removed and carefully washed with PBS to remove all the dye not attached to the cells. Once ready, samples were added to a U-bottom 96 wells microplate and incubated for 20 mins at 18°C with 100 µl of Extraction Solution (acetic acid and ethanol 50%) to extract the dye from the cells. Samples were then transferred to V-bottom 96 wells microplates and centrifuged at 1200 rpm for 10 mins at 4°C to extract the supernatant, which was then added to another V-bottom 96 wells microplate for absorbance reading. The latter was measured (Infinite M200 Pro, TECAN®) at 550 nm to detect the amount of Neutral Red dye retained by the cell's lysosomes.

2.6 Condition Index and mortality rate

As mentioned before (section 2.2.1), the condition index (CI) was evaluated to assess the physiological status of organisms before starting the experimental exposure. After acclimatization, a total of 5 organisms were randomly collected from five different tanks, and the CI was evaluated as the percentage of the ratio between the wet tissue weight (g) and the clam whole weight (g) (Silva et al., 2021).

The mortality rate of clams was also assessed in all aquaria throughout the entire experiment. MP and NP were the treatments that showed the highest mortality rate (Table 2).

Table 2: Mortality rate during the experimental exposure

Treatments	day 0	day 1-7	day 8-10	Total
CT	0	20	4	24
MP	0	28	8	36
NP	0	29	2	31
Mix	0	24	0	24

2.7 Genotoxicity Assay (Comet assay)

The level of DNA damage in clams' hemocytes was assessed as the % of DNA tail.

At the beginning of the experiment and after 7 days of exposure, 6 clams from each treatment were used to assess the level of DNA damage in hemocytes. For this purpose, the adapted comet assay protocol from (Gomes et al., 2013; Singh et al., 1988) was used. Briefly, microscopic slides were washed in ethanol/ether (1:1) prior to being coated with 0.65% normal melting point agarose (NMA) in Tris-acetate EDTA. Hemolymph was extracted from the posterior adductor muscle of each clam using a sterile hypodermic syringe (25 G needle). After collection, hemocytes were centrifuged at 3000 rpm for 3 min (4 C), and the pellets with isolated cells were then resuspended in 0.65% low melting point agarose (LMA, in Kenny's salt solution), and spread on the microscope slides in duplicate.



Figure 2.7.1: suspension of cells in LMA

For DNA immobilization and diffusion in agarose of cellular components, slides containing embedded cells were submerged in a lysis buffer (2.5 M NaOH, 100 mM EDTA, 10 mM Tris, 1% Triton X-100, 10% dimethylsulfoxide, 1% sarcosil, pH 10, 4 °C) for 1 h. After the lysis phase, slides were carefully placed in an electrophoresis solution containing electrophoresis buffer (300 mM NaOH, 1 mM EDTA, adjusted pH 13, 4 C) and electrophoresis was performed at 25 V and 300 mA for 5 minutes.

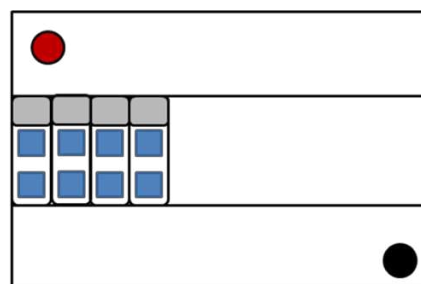


Figure 2.7.2: slides in the electrophoresis chamber

The slides were then taken out, neutralized with 0.4 mM Tris at pH 7.5, rinsed with bi-distilled water, and allowed to dry overnight.

After drying, microscope slides were stained with 20 µl of 6-diamidino-2-phenylindole (DAPI, 1 g/mL) and examined for the presence of comets with an optical fluorescence microscope (Axiovert S100) connected to a camera (Sony). Following this, to assess the quantity of DNA, the Komet 5.5 image analysis system was utilized to score 50 randomly selected cells for each slide (a total of 200 cells scored per group) at a total magnification of x400. The results are displayed as mean ± standard deviation.

Cell viability measurement:

The percentage (%) of alive cells was assessed in each sample used for Comet assay.

For this purpose, 10 µl of hemolymph were stained with 10 µl of Trypan Blue Stain 0.4% to allow cell counting. Cell viability was then measured as the percentage of alive cells in a group of 100 randomly counted cells.

2.8 Total protein evaluation

Total protein (TP) concentrations were measured in the cytosolic fraction of gills and digestive glands using the Bradford method (Bradford, 1976). The assay is a protein determination method based on the detection of changes in absorbance of the Coomassie Brilliant Blue G-250 dye. The dye interacts with proteins and changes from its double-protonated red cationic form (maximum absorbance = 470 nm) into a stable un-protonated blue form (maximum absorbance = 595 nm). The amount of bound dye and, by extension, the amount of protein in the sample is proportionate to the rise in absorbance at 590 nm. The enzymes, LPO, and AChE activities were normalized using the total protein (TP) concentrations.

Procedure:

Seven standard protein solutions were made using Bovine Serum Albumin and Milli-Q water. Previously homogenized samples were slowly defrosted on ice and gently vortexed. In a 96-well microplate, 50 µl of standards or tissue samples were pipetted in quintuplicate, and 200 µl of Bradford solution was then added to each well. Absorbance was measured at 595 nm using a microplate reader (Tecan Infinite m200-pro). The results are expressed as mg/g of wet tissue weight (w.w.).

2.9 Acetylcholinesterase (AChE) activity

AChE hydrolyzes acetylcholine to create thiocoline, which non-enzymatically interacts with 5,5'-dithiol-bis (2-nitrobenzoic acid) to produce 5-mercapto-2-nitrobenzoate (yellow). The amount of thiocoline produced and the level of AChE activity is calculated indirectly by measuring the amount of 5-mercapto-2-nitrobenzoate at 405 nm wavelength.



The activity of the enzyme acetylcholinesterase was assessed in the gills of organisms from all treatments and all sampling days (0, 7, and 10). Gills homogenates were slowly defrosted on ice. Once defrosted, 50 μ l were transferred, in triplicate, to a 96 wells microplate and incubated for 5 minutes with 200 μ l of 0.75 mM 5,5'-ditio-bis (2-nitrobenzoato) (DTNB), and then for other ten minutes with 50 μ l of 3mM acetylcholine solution (ATC) to trigger the reaction. AChE activity was then assessed following a modified protocol from Ellman's colorimetric method (Ellman et al., 1961), which indirectly measures the amount of thiocoline liberated by the reaction using the absorbance capacity (405 nm) of the final product, 5-mercapto-2-nitrobenzoato. Absorbance was read using the microplate reader Tecan Infinite m200-pro. The results are expressed in μ mol ACTC min^{-1} mg proteins $^{-1}$.

2.10 Enzymatic activities

2.10.1 Superoxide dismutase (SOD)

Superoxide dismutase catalytic activity was evaluated following the method developed by Mccords & Fridovich (1969). The latter is based on the detection, at 550 nm absorbance of the amount of reduced cytochrome *c* produced during the conversion of O_2^- (superoxide anion radical) in H_2O_2 (hydrogen peroxide) by SOD enzymatic activity.

Previously frozen (-80°C), homogenized gills and digestive glands were slowly defrosted on ice. For absorbance measurements, a spectrophotometer (JASCO V650) was used. The latter was first calibrated, filling 2 cuvettes with 2800 μ l of SOD Buffer, 100 μ l of hypoxanthine, and 100 μ l of oxidized cytochrome *c*. A xanthine oxidase test was then conducted in triplicates by adding in each cuvette 2700 μ l of SOD Buffer, 100 μ l of hypoxanthine, 100 μ l of oxidized cytochrome *c*, and 100 μ l of xanthine oxidase. The test was performed before the analyses of each group of samples belonging to the same treatment and sampling day. Following, samples were prepared for the analyses by adding 2650 μ l of SOD Buffer, 100 μ l of hypoxanthine, 100 μ l of oxidized cytochrome *c*, 50 μ l of sample, and 100 μ l of xanthine oxidase in each cuvette. The absorbance was read in triplicates at 550 nm wavelength for 1 minute. Results are expressed in $\text{U} \cdot \text{mg}^{-1} \cdot \text{prot}$.

2.10.2 Catalase (CAT)

The protocol Greenwald (1985) outlined was followed for the quantitative assessment of CAT activity. This method is based on the spectrophotometric detection of hydrogen peroxide (H_2O_2) consumption at 240 nm.

Previously frozen (-80°C), homogenized gills and digestive glands were slowly defrosted on ice. For absorbance measurements, a spectrophotometer (JASCO V650) was used. The latter was first calibrated, filling 2 cuvettes with 3 ml of CAT-buffer. Following calibration, one sample at a time was prepared for the analyses; 100 µl of each sample was added into a quartz cuvette containing 1.9 ml of CAT buffer (80 mM KH₂PO₄, 80mM K₂HPO₄) and 1000 µl of hydrogen peroxide (H₂O₂) to start the reaction. The absorbance was measured in duplicate at a wavelength of 240 nm for 1 minute. The results were expressed in units of mmol min⁻¹ mg protein⁻¹.

2.11 Lipid peroxidation

Lipid peroxidation was assessed in both gills and digestive glands for every treatment and every sampling day (0, 7, and 10) following the colorimetric method developed by (Erdelmeier et al., 1998). Previously frozen (-80°C) supernatant aliquots were slowly defrosted on ice. 200 µl of each sample was then transferred to new Eppendorf tubes and incubated in a hot bath (45°C) for 60 minutes with 650 µl of diluted 1-methyl-2-phenylindone solution and 150 µl of methanosulfonic acid solution. At the end of the incubation time, samples were centrifuged at 15 000 g and 4°C for 10 minutes to obtain a clear supernatant. In quadruplicate, 150 µl of the latter was then transferred into a 96-well microplate for absorbance measurements, performed using the microplate reader Tecan Infinite m200-pro. LPO levels are evaluated by the absorbance of malondialdehyde (MDA) and HNE (4-Hydroxynonenal) at 568 nm, and it is expressed as the amount of MDA in nmol/mg of protein.

2.12 Quality control and assessment

To avoid plastic contamination, aeration was provided using glass pipettes to prevent plastic contamination, and each tank was covered with a glass lid to prevent aerial pollution. Additionally, neither gloves nor plastic equipment/materials were used during tissue dissection to avoid further plastic contamination.

2.13 Statistical analyses

Statistically significant differences between times and treatments were evaluated according to data distribution and variance homogeneity (Shapiro-Wilk test) using parametric tests (2-way ANOVA followed by Tukey's post-hoc test) or non-parametric equivalent tests (Kruskal-Wallis and a two-tailed multiple comparison test). Only when p<0.05 results were considered statistically significant. All the statistical analyses were performed using GraphPad Prism 9.

A Principal Component Analysis (PCA) was used both for gills and digestive glands to study the relationship between treatments (control, mPE, nPS, and Mix) and between the oxidative stress and

oxidative damage biomarkers (AChE, LPO, CAT, SOD). In this case, statistical evaluations were conducted using Statistica 7.0 program.

2.14 Synergism and antagonism model

The single-dose factorial design method used was reported by Ritz et al. (2021). Gills and digestive glands were used to evaluate the presence of synergism or antagonism between nPS and mPE particles. In this method, four treatments are produced by combining two factors (the two contaminants) with two levels: control, nPS, mPE and a mixture (Mix) of the two. For all sampling days (0, 7 and 10) and all biomarkers (SOD, CAT, LPO, AChE and DNA damage) values were evaluated using the following dose addition and independent action models. Dose addition defines the reference effect (when neither synergism nor antagonism occurs) as the sum of the variance of treatments compared to controls:

$$E_{add} = (E_{nPS} - E_{control}) + (E_{mPE} - E_{control}) \quad (1)$$

The difference between the observed effect of the mixture of the two contaminants ($E_{Mix} - E_{control}$) and the predicted response (E_{add}) defines the presence of either antagonistic or synergistic effect:

$$D_{da} = E_{Mix} - E_{control} - E_{add} = E_{Mix} - E_{nPS} - E_{mPE} + E_{control} \quad (2)$$

Independent action defines the reference effect as the product between the variance of treatments compared to controls:

$$E_{ind} = E_{control} \left(1 - \frac{E_{control} - E_{nPS}}{E_{control}}\right) \left(1 - \frac{E_{control} - E_{mPE}}{E_{control}}\right) = \frac{E_{nPS} \cdot E_{mPE}}{E_{control}} \quad (3)$$

Alike dose addition, any antagonistic or synergistic effect can be defined as the difference between the observed (E_{Mix}) and the predicted response (E_{add}):

$$D_{ia} = E_{Mix} - \left(\frac{E_{nPS} \cdot E_{mPE}}{E_{control}}\right) \quad (4)$$

A synergistic effect is observed when D_{da} and D_{ia} are larger than zero; otherwise (<0), an antagonistic effect exists.

Results of synergistic and antagonistic impacts are valuable only for the concentrations used during the experiment (10 $\mu\text{g/L}$ of mPE, 10 $\mu\text{g/L}$ of nPS, 10+10 $\mu\text{g/L}$ of mPE + nPS).

2.15 Weight of Evidence (WOE)

The Weight of Evidence (WOE) quantitative model was used to integrate the set of data, line of Evidence (LOE), obtained from biomarkers analyses (AChE, DNA damage, CAT, LPO, SOD) conducted on gills and/or digestive glands. This approach is used to simply further results interpretations and obtain more robust and weighted conclusions (Regoli et al., 2019).

Briefly, a percentage of variation is calculated for each biomarker individually. Single values are then normalized/corrected by comparing them with their specific threshold (level of variation above which there is biological relevance), weight (toxicological relevance), and statistical differences with controls, with the final creation of classes of effects (Regoli et al., 2019).

Whole calculations, detailed flow charts, the rationale for weights, thresholds, and expert judgments have been previously described in detail (Regoli et al., 2019)

3-RESULTS

3.1 nPS and mPE characterization

Analyses on nPS (50 nm) hydrodynamic diameter in ultrapure water show that over time the particles are stable (ζ -potential= -68.8 ± 0.66 mV), and their size does not vary, thus meaning that in those conditions, no aggregation is observed (Fig. 3.1.1). nPS were also analyzed in a mixture with mPE (4-6 μ m) through laser diffraction analyses. In this case, the average results on particle size distribution showed a high level of aggregation, in fact, no particles smaller than 3 μ m were found (Fig. 3.1.2). This is probably due to an aggregation of the nPS with the mPE present in the solution, demonstrated by the highest presence of particles with a size between 8 and 9 μ m, size of the mPE used.

On the other hand, laser diffraction analyses on mPE (4-6 μ m) show a certain level of aggregation even when mPE particles are tested alone. In fact, the highest percentage was found for particles between 4 and 6 μ m (mPE fabrication size) but also for particles up to 118 μ m (Fig. 3.1.3). However, as for nPS, when particles are tested in the mixture (nPS + mPE suspension) a higher level of aggregation even for mPE is observed. This is demonstrated by the presence of a high %volume only for particle sizes bigger than 100 μ m to 625 μ m (Fig. 3.1.4).

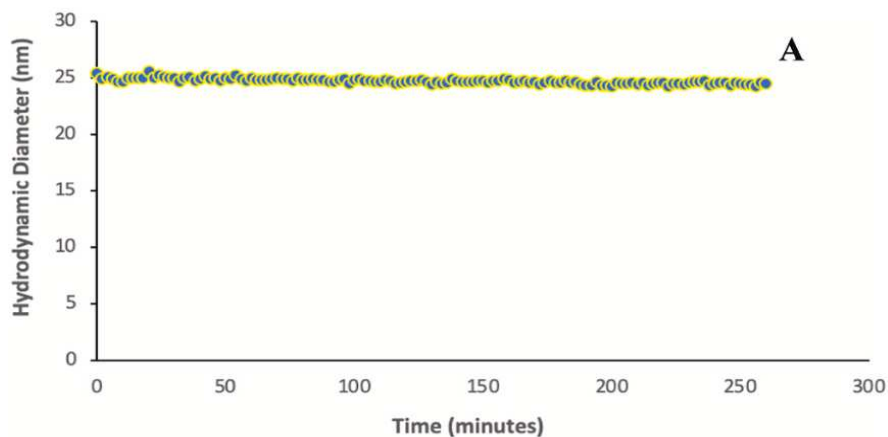


Figure 3.1.1: Hydrodynamic diameter of polystyrene nanoplastics (50nm) in ultrapure water

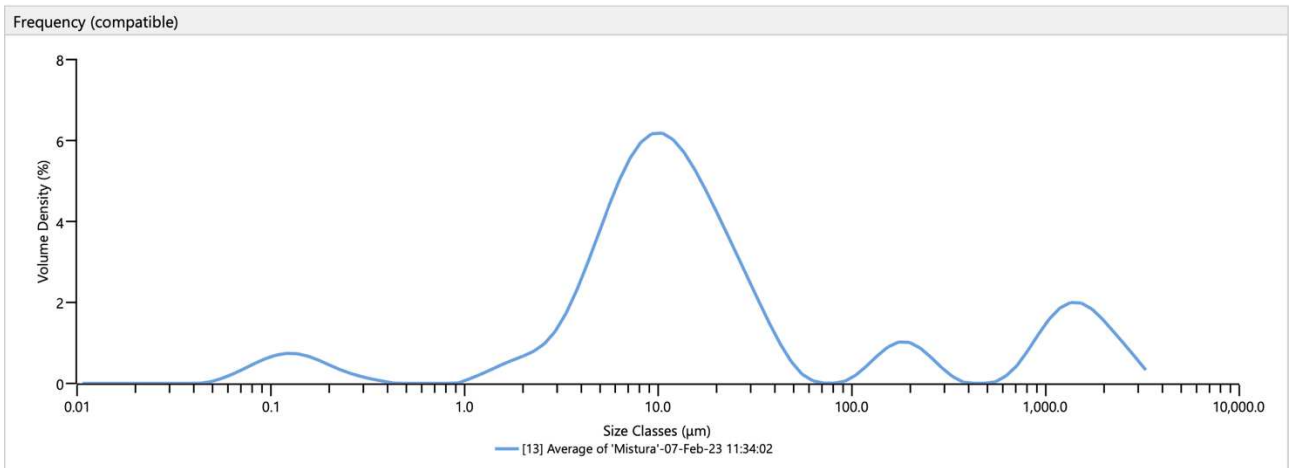


Figure 3.1.2: Average PSD obtained from laser diffraction analyses on nPS (50 nm) in a mixture with mPE (4-6 μm).

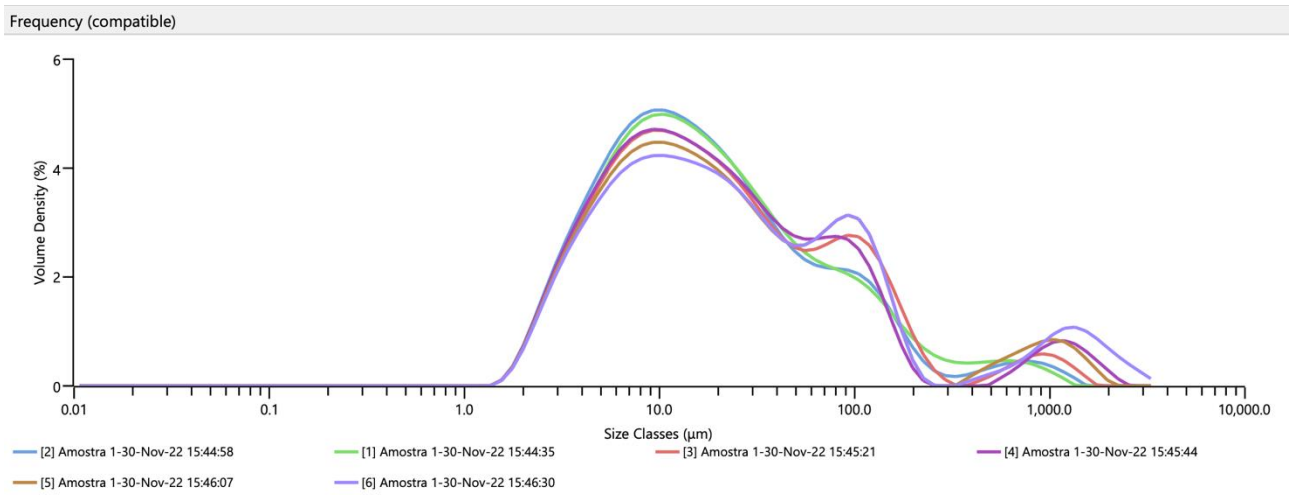


Figure 3.1.3: PSD results from laser diffraction analyses on mPE (4-6 μm).

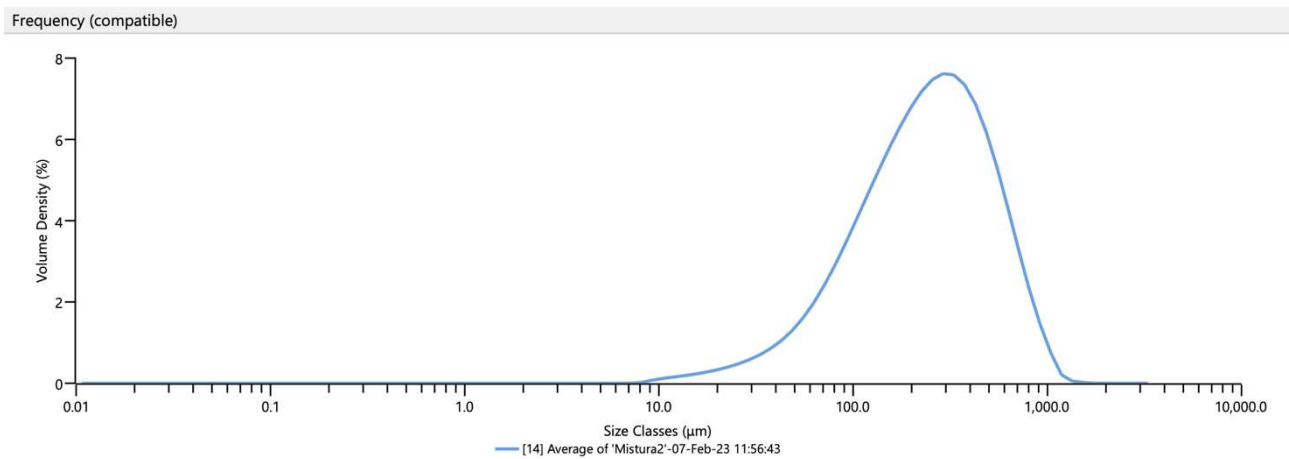


Figure 3.1.4: Average PSD obtained from laser diffraction analyses on mPE (4-6 μm) in a mixture with nPS (50 nm).

3.2 Ingestion

For clams exposed to nPS and Mix treatments, both gills and digestive glands show a significant increase in the amount of ingested nPS particles between day 0 and day 10 ($p < 0.05$) with similar levels of ingestions for both tissues (Fig 3.2.1 A and B).

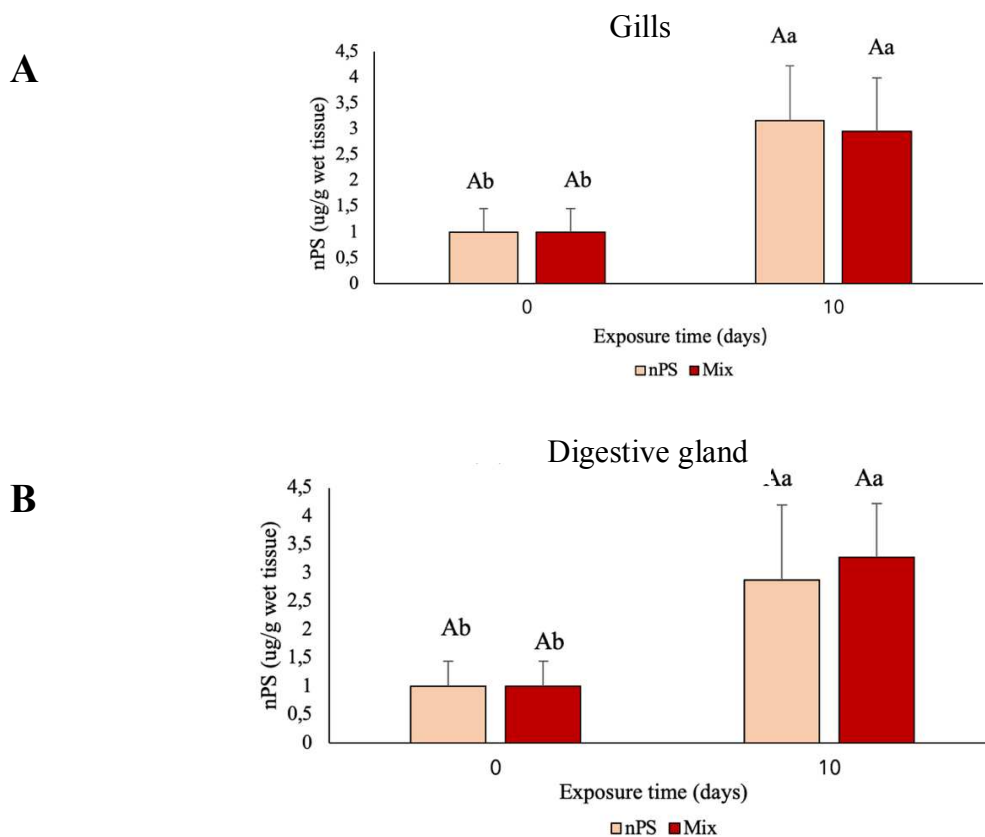


Fig.3.2.1 amount of nanoplastics detected in the gills of clams expressed as μg of nanoplastic/ μg of wet tissue (A); amount of nanoplastics detected in the digestive gland of clams and expressed as μg of nanoplastic/ μg of wet tissue (B). Significant variations between treatments at the same time and between times for the same treatment are indicated, respectively, by different upper- and lower-case letters ($p < 0.05$).

In relation to mPE ingestion, both in gills and DG particles were not detected in CT (Figure 3.2.2 A and B). For mPE and Mix exposed organisms, a similar level of particle ingestion was observed for both treatments and tissues (gills and digestive glands) (Figure 3.2.2 A and B).

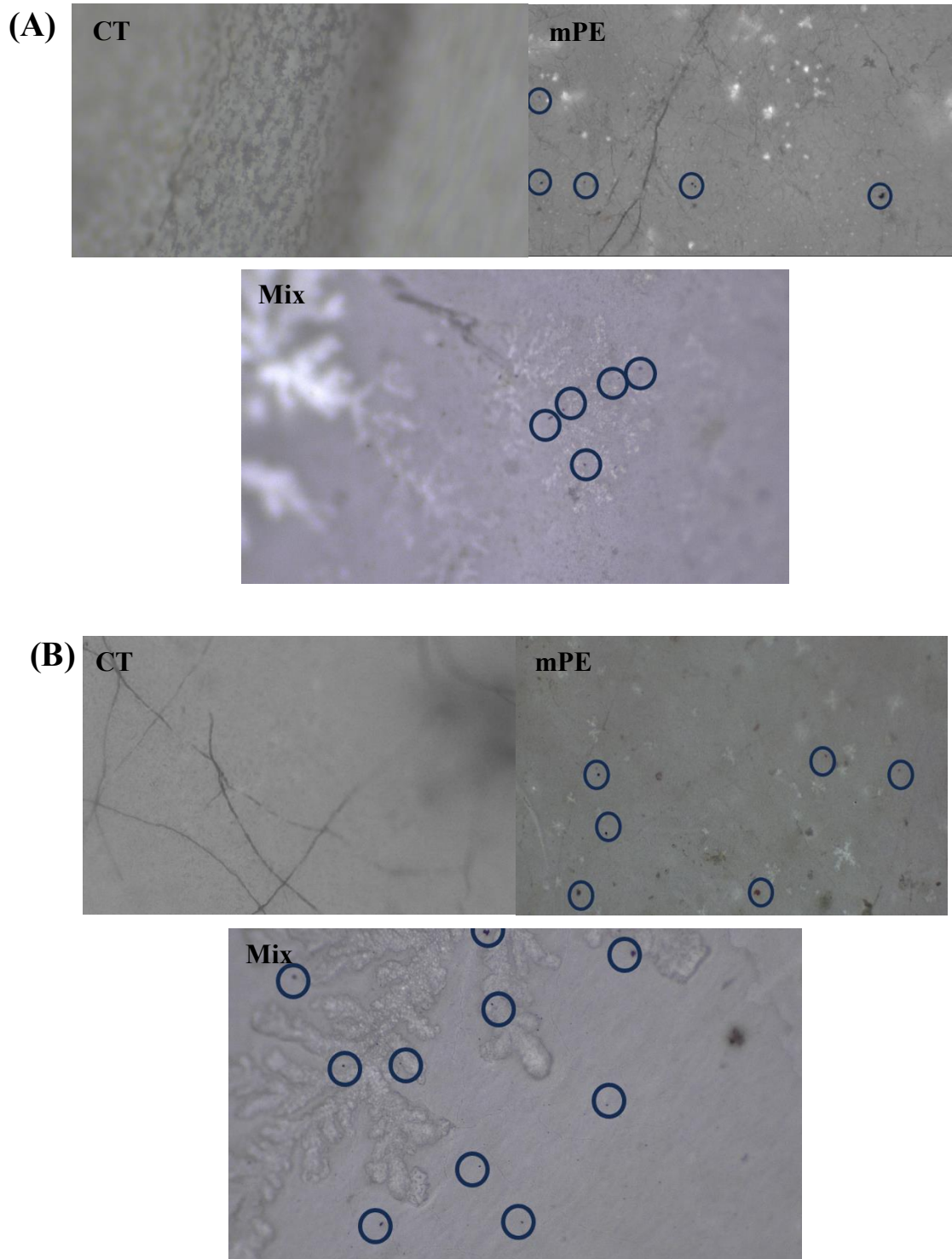


Figure 3.2.2 mPE ingestion in gills of unexposed (CT), mPE and Mix exposed *R. decussatus* after 10 days (A); mPE ingestion in digestive glands of unexposed (CT), mPE and Mix exposed *R. decussatus* after 10 days (B). Blue circles highlight mPE particles found in samples.

3.3 In vitro assay

Results show a significant increase in the number of alive hemocytes cells after a 24 h exposure to nPS treatment ($p < 0.05$) (Fig. 3.3.1).

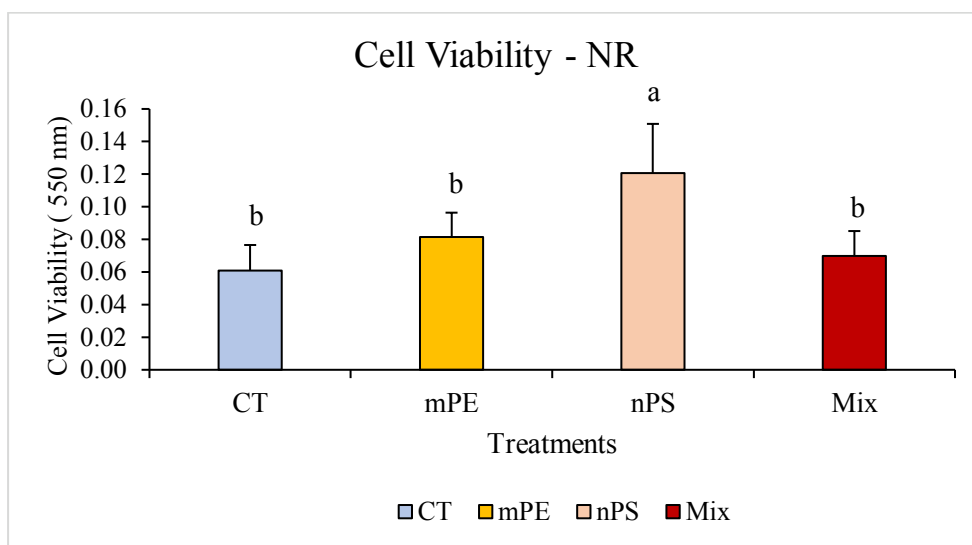


Figure 3.3.1: Differences in cell viability (Neutral Red dye) between *Ruditapes decussatus* unexposed hemocytes (CT), 24 h mPE (10 $\mu\text{g/L}$) exposed hemocytes, 24 h nPS (10 $\mu\text{g/L}$) exposed hemocytes, and 24 h Mix (10 $\mu\text{g/L}$ mPE + 10 $\mu\text{g/L}$ nPS) exposed hemocytes. Different letters indicate significant differences between treatments ($p < 0.05$).

3.4 Condition Index and mortality rate

Before starting the experimental exposure, the good physical status of organisms was assessed by comparing CI values calculated by Silva et al., 2021 in organisms of *Ruditapes decussatus* collected in the Ria Formosa lagoon during summertime and CI values calculated in this study (31.6 ± 1.7).

3.5 Genotoxicity assay (Comet assay)

As shown in Fig. 3.5.1 (A), there is no significant difference between days 0 and 7 for all treatments ($p < 0.05$) (control, mPE, nPS, Mix), indicating that no DNA damage occurred. However, a significant decrease in the % of DNA tail was found at day 7 for nPS and Mix treatment when compared to unexposed and mPE-exposed clams ($p < 0.05$). Examples of comets in clams' hemocytes are shown in Fig. 3.5.1 (B); in accordance with Fig. 3.5.1 (A), the level of DNA damage does not vary significantly except for the nPS and mPE treatment at day 7, where nuclear core with a significant decrease in the amount of DNA migrating into the tail is observed.

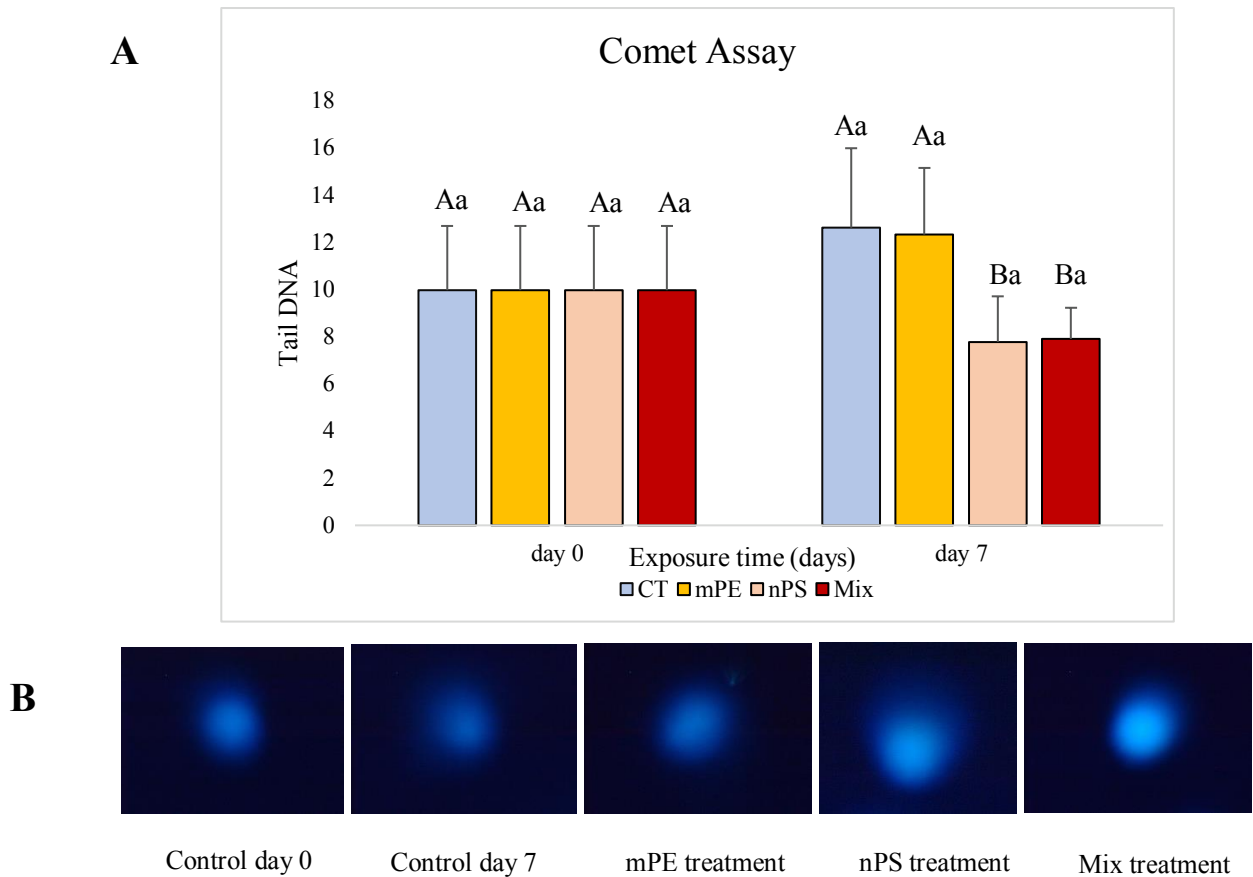


Fig. 3.5.1 Variation in the level of DNA damage (mean \pm sd) between different treatments (CT, mPE, nPS, Mix) and different days of exposure (0 and 7) in *Ruditapes decussatus* (A). Examples of comets in hemocytes of clams from all treatments (B). Significant variations between treatments at the same time and between times for the same treatment are indicated, respectively, by different upper- and lower-case letters ($p < 0.05$).

3.6 Neurotoxicity assay (Acetylcholinesterase (AChE) activity)

Differences in AChE activity were found in clams' gills between different treatments at day 7 and day 10 (Fig. 3.6.1). More in detail, at day 7, there is a significant change in AChE activity between control, mPE, and nPS treatments ($p < 0.05$), where the highest activity is seen for clams exposed only to mPE whilst the lowest value is noticeable for organisms exposed only to nPS (Fig. 3.6.1). On the other hand, at day 10 there is a significant increase in AChE enzymatic activity for the Mix treatment when compared to the others (CT, mPE, and nPS) ($p < 0.05$) (Fig. 3.6.1).

Comparing the same treatments but at different times (0,7 and 10), a significant increase in neurotoxicity is observed for both CT and mPE treatments at day 7 compared to days 0 and 10 (Fig. 3.6.1) and for clams exposed to nPS and Mix treatments at day 10 compared to day 0 and 7 ($p < 0.05$) (Fig. 3.6.1).

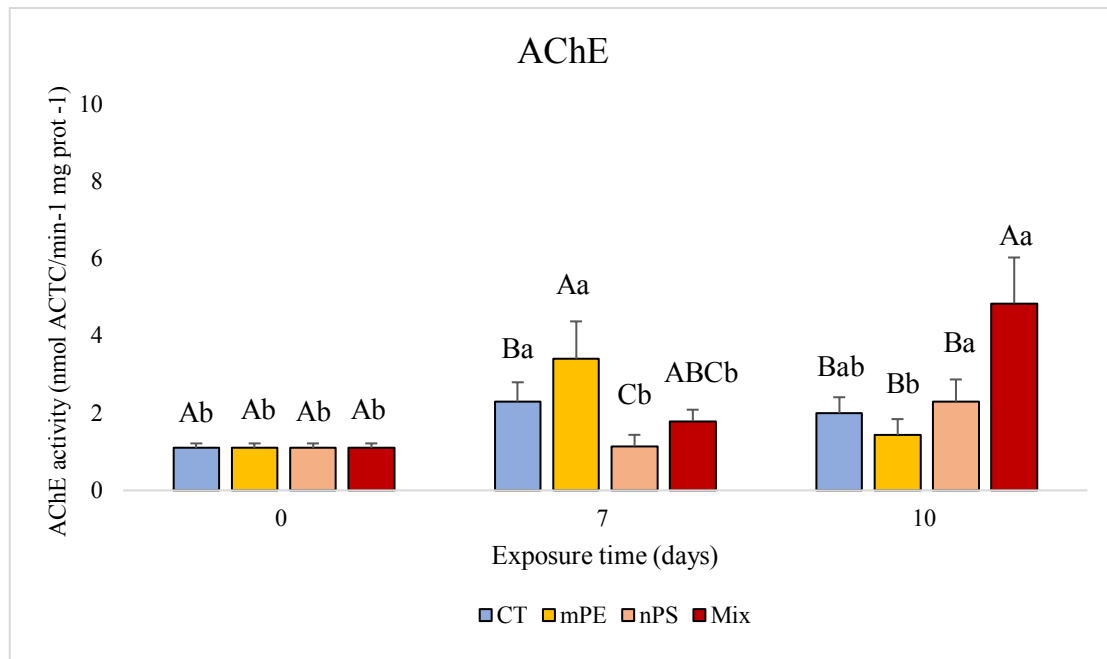


Fig. 3.6.1 AChE enzymatic activity in gills of *Ruditapes decussatus* at different times of exposures (0, 7, and 10) and between different treatments (CT, mPE, nPS, and Mix). Significant variations between treatments at the same time and between times for the same treatment are indicated, respectively, by different upper- and lower-case letters ($p < 0.05$).

3.7 Enzymatic activities

Changes in the activity of antioxidant enzymes (SOD and CAT) are presented in this section. Results are discussed separately based on the tissue (gills and digestive gland).

3.7.1 Superoxide dismutase (SOD)

In the gills of *Ruditapes decussatus* exposed mPE particles, SOD activity at day 10 is significantly higher compared to the control and compared to day 0 and day 7 ($p < 0.05$) (Fig. 3.7.1 A).

In digestive glands, SOD activity significantly increases after 10 days of exposure to mPE, nPS, and Mix treatments ($p < 0.05$) (Fig. 3.7.1 B). Furthermore, at day 10, increased activity is observed for organisms exposed separately to mPE and nPS compared to unexposed ones ($p < 0.05$) (Fig. 3.7.1 B), where the highest augmentation is seen in relation to the nPS treatment (Fig. 3.7.1 B).

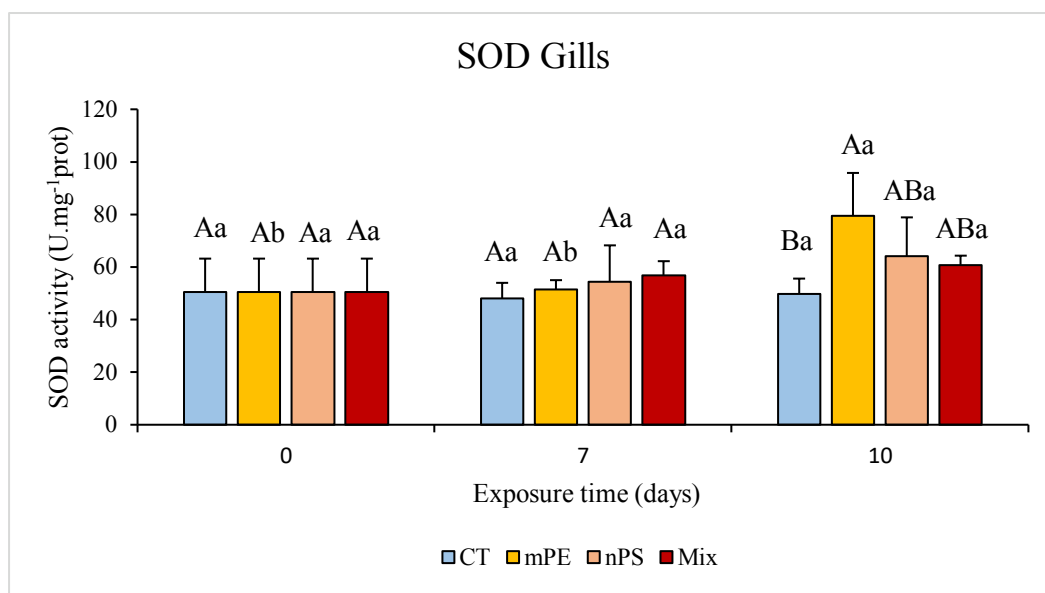
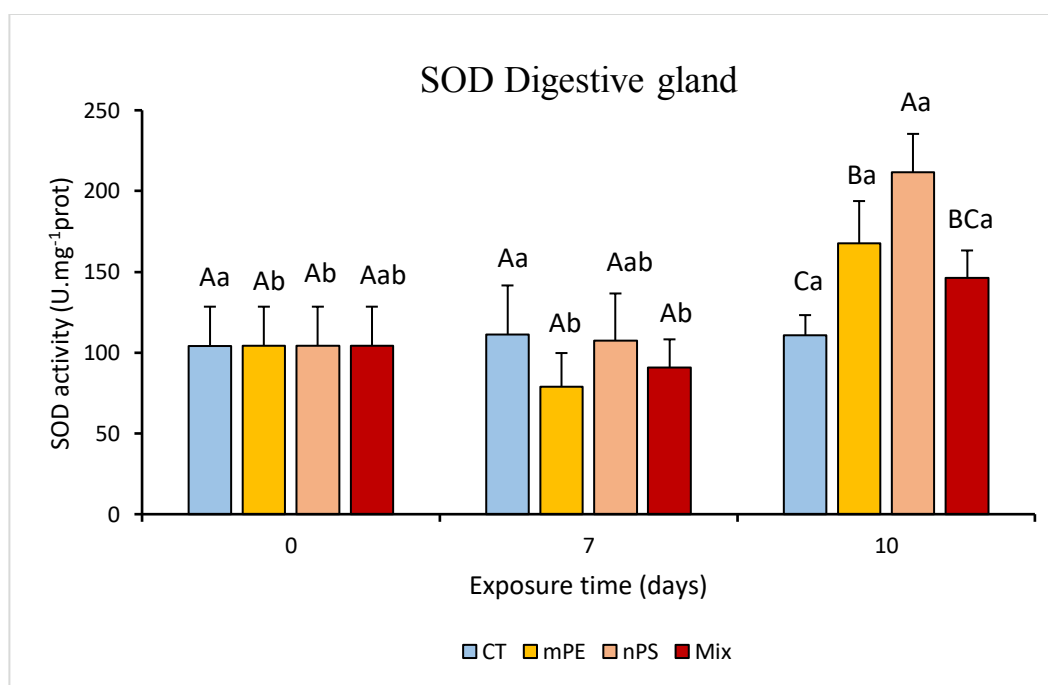
A**B**

Fig. 3.7.1 SOD activity changes in the gills (**A**) and digestive gland (**B**) of *Ruditapes decussatus* between different treatments (CT, mPE, nPS, Mix) and different times of exposure (0, 7, and 10). Significant variations between treatments at the same time and between times for the same treatment are indicated, respectively, by different upper- and lower-case letters ($p < 0.05$).

3.7.2 Catalase (CAT)

Gills results for changes in CAT activity are presented in Fig. 3.7.2 A. No significant changes are observed between treatments both at day 0 and 7 ($p > 0.05$) (Fig. 3.7.2 A); nevertheless, at day 10, a major increase of the enzymatic activity was observed for nPS, and Mix treatments compared to the control ($p > 0.05$). The highest activity is seen after 10 days of exposure for organisms exposed to the Mix (Fig. 3.7.2 A).

Also, in the digestive gland, no significant differences were found between day 0 and day 7 for all treatments ($p>0.05$) (Fig. 3.7.2 B); however, on day 10, a statistically significant increase in CAT activity compared to day 0 and day 7 is observed for clams exposed to mPE and to Mix treatments ($p>0.05$) (Fig. 3.7.2 B). The highest increase is seen after 10 days of exposure to mPE (Fig. 3.7.2 B).

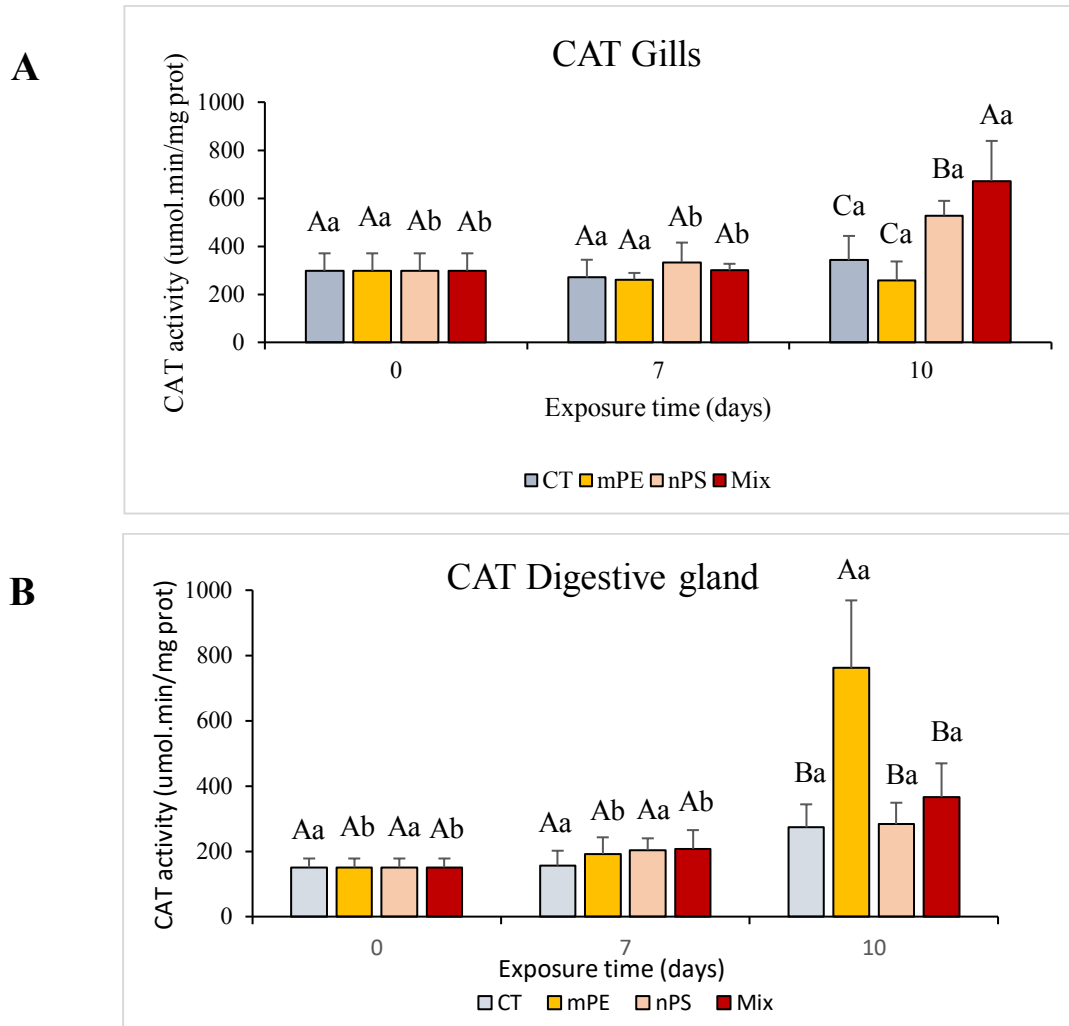


Fig. 3.7.2 Catalase activity changes in gills (**A**) and digestive glands (**B**) of *Ruditapes decussatus* between different treatments (CT, mPE, nPS, Mix) and different times of exposure (0, 7, and 10). Significant variations between treatments at the same time and between times for the same treatment are indicated, respectively, by different upper- and lower-case letters ($p < 0.05$).

3.8 Lipid peroxidation

In gills, no variations in MDA levels are observed for all treatments (CT, mPE, nPS, Mix) at days 0 and 7, while a significant decrease in the level of oxidative damage was seen at day 10 for organisms exposed to mPE compared to CT and nPS treatments and compared to day 0 and 10 ($p>0.05$) (Fig. 3.8.1 A).

As shown in Fig. 3.8.1 (B), also in the digestive gland of analyzed clams, we have no variation in MDA levels, although a significant decrease ($p < 0.05$) is seen for the nPS treatment between sampling days 0 and 7 (Fig. 3.8.1 B).

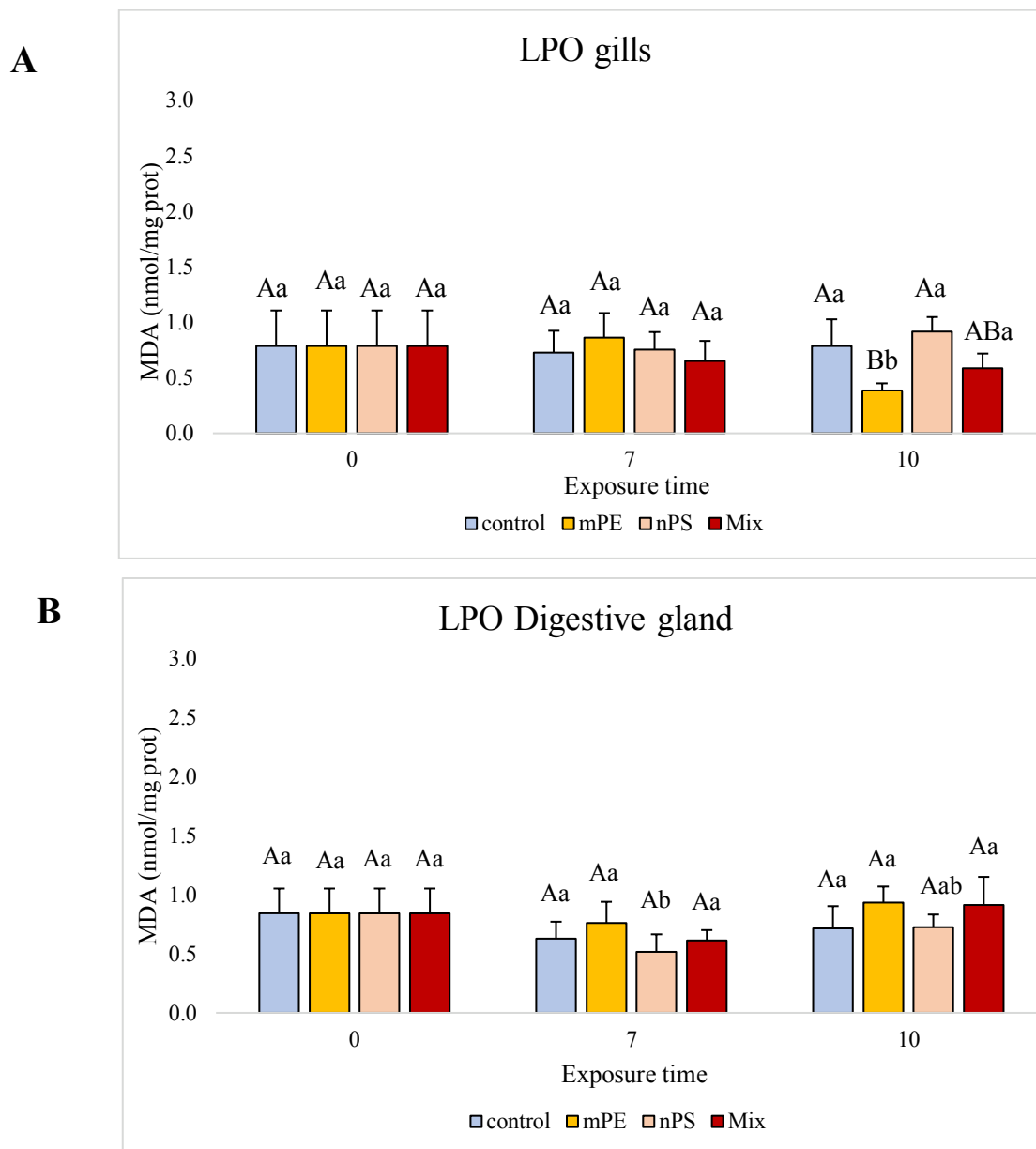


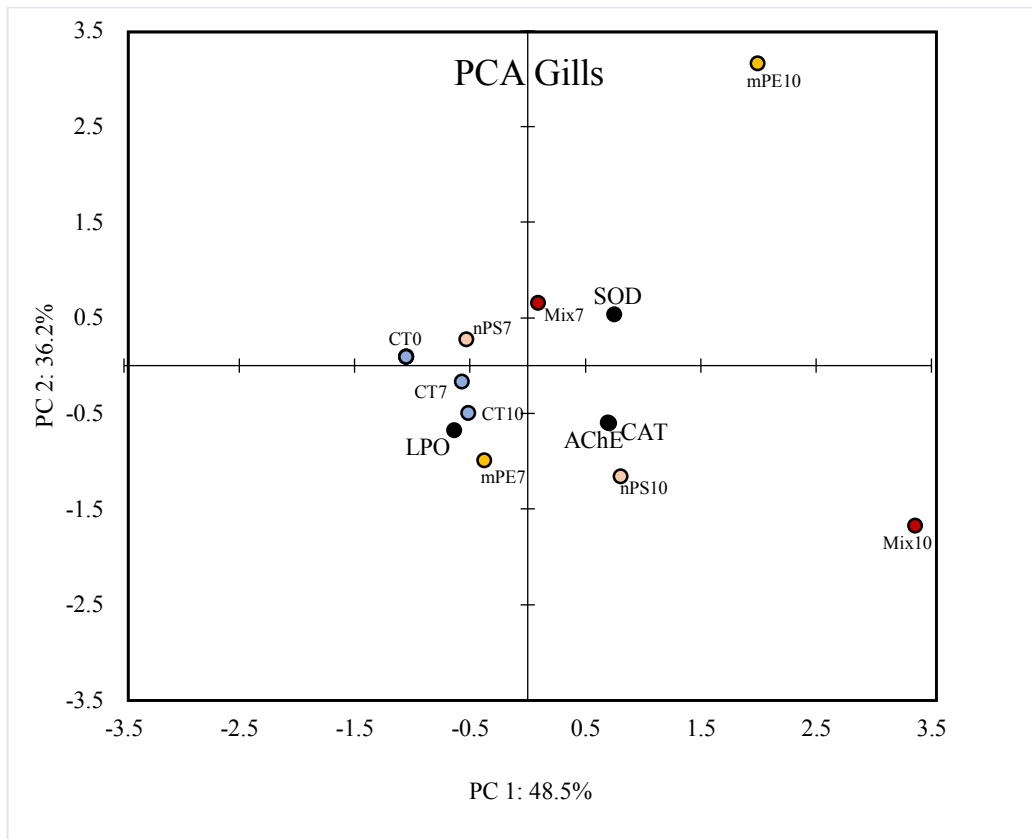
Fig. 3.8.1: LPO levels changes in gills (A) and digestive glands (B) of clams from different treatments (CT, mPE, nPS and Mix) and different days of exposure (0, 7, and 10). Significant variations between treatments at the same time and between times for the same treatment are indicated, respectively, by different upper- and lower-case letters ($p < 0.05$).

3.9 PCA

To further understand the effects of nPS, mPE, and their mixture on biomarker responses, a principal component analysis (PCA) was applied. The two principal components represent 84.7% in the gills (PC1 = 48.5%, PC2 = 36.2%) and 87.3% in the digestive glands of clams (PC1 = 61.5, PC2 = 35.8%) of the total variance (Fig. 3.9.1 A and B). Overall results suggest a time-specific effect in both clam tissues, whereby day 10 is most influential (Fig. 3.9.1 A and B). In the clam's gills, SOD,

CAT, and AChE are the most influential biomarkers relative to the observed effects, as is the exposure to the Mix and mPE (Fig. 3.9.1 A). In the digestive gland of clams, mPE particles are the most prominent treatment, with LPO, CAT, and SOD having a powerful effect on the results observed (Fig. 3.9.1 B). These PCA descriptive analyses suggest that the clam's digestive gland is the most compromised tissue compared to the gills and that the Mix and mPE are most influential on biomarker responses compared to nPS (Fig. 3.9.1 A and B).

A



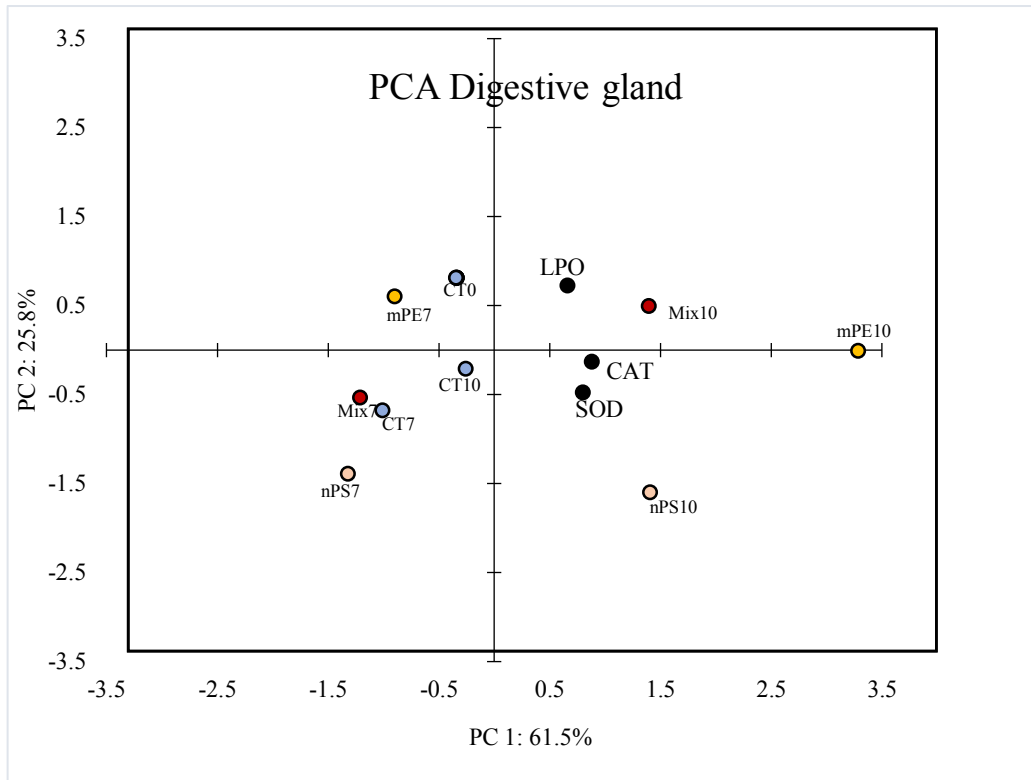
B

Figure 3.9.1: Principal component analysis (PCA) of a battery of biomarkers (CAT, SOD, LPO, AChE) in gills (A) and digestive glands (B) of *Ruditapes decussatus* for all treatments (CT, mPE, nPS, Mix) and all sampling days (0, 7, 10).

3.10 Synergism and Antagonism

3.10.1 Dose addition results:

In the gills of *Ruditapes decussatus*, an increasing antagonistic interaction ($D_{da} < 0$) is observed in relation to SOD enzymatic activity between days 7 and 10 (Table 3). Considering CAT, synergism ($D_{da} > 0$) at day 7 and antagonism ($D_{da} < 0$) at day 10 are observed (Table 3). No interaction ($D_{da} \approx 0$) was detected for LPO, neurotoxicity, and genotoxicity (Table 3).

Table 3: Dose addition results for the synergistic and antagonistic interactions between mPE and nPS in gills (SOD, CAT, LPO, neurotoxicity) and hemolymph (genotoxicity) of *Ruditapes decussatus*.

Exposure time (days)	SOD	CAT	LPO	Neurotoxicity	Genotoxicity
0	0	0	0	0	0
7	-6	43	0	-2	9
10	-26	-59	1	-2	

On the other hand, in digestive glands, a decreasing synergistic interaction ($D_{da}>0$) for SOD activity and an increasing antagonistic interaction ($D_{da}<0$) for CAT activity is observed between days 7 and 10 (Table 4). Neither synergism nor antagonism is observed for LPO (Table 4).

Table 4: Dose addition results for the synergistic and antagonistic interactions between mPE and nPS in digestive glands (SOD, CAT, LPO) of *Ruditapes decussatus*.

Exposure time (days)	SOD	CAT	LPO
0	0	0	0
7	49	-40	0
10	8	-571	0

3.10.2 Independent action results:

When considering E_{ia} as the reference value, gills show the presence of antagonism ($D_{ia}<0$) in relation to SOD on day 10 and to CAT on day 7 (Table 5). Synergistic interactions ($D_{ia}>0$) occur for CAT on day 10 (Table 5). No interactions ($D_{ia}\approx 0$) are observed for LPO, neurotoxicity, and genotoxicity.

Table 5: Independent action results for the synergistic and antagonistic interactions between mPE and nPS in gills (SOD, CAT, LPO, neurotoxicity) and hemolymph (genotoxicity) of *Ruditapes decussatus*.

Exposure time (days)	SOD	CAT	LPO	Neurotoxicity	Genotoxicity
0	0	0	0	0	0
7	-1	-24	0	0	0
10	-42	273	0	3	

Also, in digestive glands, an antagonistic interaction ($D_{ia}<0$) is observed for SOD at day 10 (Table 6). In relation to CAT, an increasing antagonistic interaction is observed between days 7 and 10 (Table 6). No interactions ($D_{ia}\approx 0$) are present for LPO oxidative damage (Table 6).

Table 6: Independent action results for the synergistic and antagonistic interactions between mPE and nPS in digestive glands (SOD, CAT, LPO) of *Ruditapes decussatus*.

Exposure time (days)	SOD	CAT	LPO
0	0	0	0
7	15	-42	0
10	-174	-423	0

3.11 Weight of Evidence

The overall WOE elaboration of biomarker results (AChE, LPO, CAT, SOD) shows a time-related response, whereby for nPS, mPE, and Mix treatments, the highest level of hazard is observed at sampling day 10 (Fig. 3.11.1). CAT activity in gills and SOD activity in digestive glands are the biomarkers that mostly contribute to the overall increase of hazard at sampling day 10.










Sample code	N. param in class ABSENT	N. param in class SLIGHT	N. param in class MODERATE	N. param in class MAJOR	N. param in class SEVERE	Level of hazard for biomarker	
Mix_0	8	0	0	0	0	ABSENT	
Mix_7	7	0	0	0	0	ABSENT	
Mix_10	5	1	1	1	0	MODERATE	
mPE_0	8	0	0	0	0	ABSENT	
mPE_7	8	0	0	0	0	ABSENT	
mPE_10	3	0	3	0	1	MODERATE	
nPS_0	8	0	0	0	0	ABSENT	
nPS_7	7	0	1	0	0	SLIGHT	
nPS_10	5	0	1	1	0	MODERATE	

Figure 3.11.1: Weight of Evidence (WOE) in relation to nPS, mPE, and Mix treatments and sampling days 7 and 10.

4-DISCUSSION

Repercussions of plastic pollution on the entire ocean ecosystem are of great concern nowadays. Indeed, with the increasing world population and GPP, the amount of plastic entering the ocean is growing along with the detection of smaller plastic fragments (MPs and NPs). Combining both

primary and secondary sources of plastic particles, it was estimated that 5.25 trillion fragments are currently polluting the global sea surface most of which are less than 10 mm in size (Alimi et al., 2018). There is evidence that once MPs and NPs enter the marine environment, they can form aggregates due to their interaction with seawater components (e.g., colloids, algae, ions) and other dispersed plastic particles of equal or similar size, that change their chemical/physical properties, structure, and size, potentially influencing their level of toxicity, bioavailability, fate, and transport (Abdul Rahman et al., 2023; Gonçalves et al., 2022; Gonçalves & Bebianno, 2021; Li et al., 2019). Taking this into account, this study aims to assess how the occurrence of possible interactions between nPS (50 nm) and mPE (4-6 μm) when in a mixture with each other, can positively or negatively influence the particles' toxicological hazard towards the clam *Ruditapes decussatus*.

According to Alimi et al. (2018), the phenomenon of particle attachment after a collision is known as "aggregation". The process is controlled by Van der Waals and electrical double-layer forces and can be furthermore influenced by diffusion and particles' surface charge properties (Alimi et al., 2018). The characterization of plastics in ultrapure water indicates that nPS are less prone to form aggregates compared to mPE (Fig. 3.1.1 and Fig. 3.1.3). This is consistent with earlier data by Gonçalves et al. (2022) and Shams et al. (2020), in which analyzed NPs did not aggregate in ultrapure water because of the repelling forces between their negatively charged surfaces. As PE, by nature, is a non-polar polymer, while PS was seen to enhance its negativity due to the dissociation of functional groups (Shams et al., 2020), the increased MPs tendency to aggregate (Fig. 3.1.3) identified in this study may be attributable to differences in the polymers used. Interestingly, when analyzed in a mixture with each other, both NPs and MPs showed, in ultrapure water, a higher level of aggregation (Fig. 3.1.2 and Fig 3.1.4). Indeed, nPS and mPE suspended together were seen to form aggregates of a size up to 10 μm and between 100 and 1000 μm , respectively (Fig. 3.1.2 and Fig 3.1.4). This may be explained by variations in surface charge energy, higher for MPs compared to NPs (H. Sun et al., 2021), which reduce repulsive attractions and favour higher attachment probabilities between MPs and NPs compared to particles of equal sizes. When analyzed in seawater, aggregation of MPs and NPs was found to be higher compared to ultrapure water (Gonçalves et al., 2022; H. Sun et al., 2021). It is possible that this is connected to the breakdown of energy barriers between particles caused by an increase in ionic strength (IS), which is strictly dependent on the rising concentration of sodium chloride (NaCl) (Alimi et al., 2018; Shams et al., 2020). In fact, free ions present in seawater can be absorbed by plastic particles changing their surface charges properties and allowing them to form aggregates (Abdul Rahman et al., 2023; Gonçalves & Bebianno, 2021; Li et al., 2019). When taking this into account, it is possible to forecast that, in a more environmentally realistic condition, when MPs and NPs are dispersed together in seawater, they might present an even higher level of

aggregation compared to the one observed here in ultrapure water. This could significantly affect their mobility, persistency, and bioavailability in the environment (Alimi et al., 2018; Gonçalves & Bebianno, 2021).

Up to date, many studies have been investigating how smaller plastic fragments might be more easily ingested by marine organisms, potentially causing a higher toxicological hazard (Baudrimont et al., 2020; Gonçalves & Bebianno, 2021; Rodrigues et al., 2022; Wang et al., 2021; Ward et al., 2019). In accordance, a high level of ingestion was obtained for both tissues analyzed (gills and digestive gland) after 10 days of exposure of *Ruditapes decussatus* to individual mPE and nPS (Fig. 3.2.1 A & B and Fig. 3.2.2 A & B). Recently, also Gonçalves et al. (2023) found a high level of ingestion in *Mytilus galloprovincialis* exposed for 28 days to nPS (50 nm). Moreover, also in wild bivalves species, a high accumulation of smaller plastic fragments was found (Abidli et al., 2019; Cozzolino et al., 2021).

Interestingly, elevated ingestion was also observed here for organisms exposed to the Mix treatment (Fig. 3.2.1 A & B and Fig. 3.2.2 A & B), where particles were seen to form bigger aggregates (Fig. 3.1.2 and Fig 3.1.4). The initial step in bivalves feeding processes is particle capture, which results from contacting and retaining gills filaments (Rosa et al., 2018). Pre-ingestion capture efficiency (CE) was found to rise asymptotically as particle size increases (Ward et al., 2019). Therefore, the higher efficiency in trapping larger particles in the gills may account for the high ingestion found here in the gills of *R. decussatus* exposed to the Mix treatment (Fig. 3.2.1 A and Fig. 3.2.2 A). Despite evidence that post-capture selection mechanisms, such as gills' muscular contraction, can allow bivalves to finally ingest smaller particles and reject bigger ones (Ward et al., 2019), foraging theories suggest that for suspension-feeding organisms might be more advantageous in terms of food value, to ingest also larger phytoplanktonic cells (Ward & Shumway, 2004). Indeed, several data showed how pre-ingestion selection of filtered material most of the time is not based on particles sizes but on other characteristics, such as the physiochemical properties (e.g., particle's charge and hydrophobicity) of the particle that interacts with the feeding organs (Rosa et al., 2017, 2018; Ward et al., 2019). When considering this, along with the higher CE of bigger particles (Ward et al., 2019) and the higher filtration rate observed for *R. decussatus* compared to other suspension feeders (Abidli et al., 2019; Cozzolino et al., 2021; Sobral & Widdows, 2000), it can be concluded that the likelihood of ingesting bigger aggregates is high for this organism. This might explain the high level of ingestion observed here in the digestive gland of *R. decussatus* exposed to the Mix treatment (Fig. 3.2.1 B and Fig. 3.2.2 B). For example, Abidli et al. (2019) and Cozzolino et al. (2021) found that most ingested particles by wild specimens of *R. decussatus* were in the range of mm. Nonetheless, further analyses should be conducted on ζ -potential values of the aggregates formed when MPs and NPs are suspended together to better understand results.

Once ingested, plastic particles can either accumulate in the digestive tract or can be translocated in hemolymph or other tissues (Fossi et al., 2018; Sendra et al., 2021; Sikdokur et al., 2020; Wang et al., 2021). This study used the neutral red uptake assay to quantitatively assess changes in cell viability of hemocytes subjected to a 24 h *in vitro* exposure to mPE, nPS, and Mix. This method is based on the ability of viable cells to incorporate and bind neutral red dye in lysosomes (Repetto et al., 2008). nPS was the only treatment to cause significant changes, increasing hemocytes cell viability (Fig. 3.3.1). Such an effect might be related to higher localized toxicity of nPS towards lysosomes, as stated by Repetto et al. (2008) that chemically localized effects on lysosomes can also result in a higher neutral red dye uptake. In accordance with this, it has been reported that once ingested, NPs, due to their smaller sizes, are able to more easily cross biological membranes (Gonçalves & Bebianno, 2021; Kiran et al., 2022), possibly accumulating in lysosomes (Zhou et al., 2023) and reducing their membrane stability (Capolupo et al., 2021). Furthermore, a higher level of NPs accumulation in lysosomes compared to MPs was observed by Gaspar et al. (2018), possibly explaining the absence of effects observed here for hemocytes exposed to mPE and Mix treatments (Fig. 3.3.1).

Free radicals can be defined as highly reactive molecules due to their presence of unpaired electrons in atomic orbitals (Bounous & Molson, 2003). This unstable state favors the free radical reactions with other molecules by either donating or subtracting electrons to reach stability (Bounous & Molson., 2003). Since oxygen is the final acceptor of electrons in the mitochondrial electron transport chain, most free radicals in aerobic organisms are produced from oxygen during metabolic respiration (Bounous & Molson, 2003; Abele & Puntarulo, 2004). Reactive oxygen species (ROS), such as superoxide anions ($O_2^{\circ-}$), hydroxyl radicals ($^{\circ}OH$), and hydrogen peroxide (H_2O_2), are intermediates of the 4-electron oxygen reduction present in the water molecule (Abele & Puntarulo, 2004) and their formation, if not maintained under control, might present detrimental effects on many biological structures (Benedetti et al., 2022). As an evolutionary consequence, organisms developed antioxidant defense systems to eliminate metabolic ROS formation (Bounous & Molson, 2003). Moreover, organisms' exposure to emerging environmental contaminants, such as NPs and MPs, was seen to potentially increase ROS production, thus altering antioxidant defense mechanisms and inducing, in many cases, oxidative damage (lipid peroxidation, protein oxidation, DNA damage, and unbalance of intracellular redox status) (Benedetti et al., 2022). Taking this into account, a multi-biomarker approach was used to study different genotoxic (% of DNA tail), neurotoxic (AChE), oxidative stress (SOD, CAT), and oxidative damage (LPO) responses in relation to different plastic particles sizes. Different times and tissues were also considered to further understand possible time and tissue-dependent effects.

The first line of the enzymatic antioxidant defense system in bivalves is represented by the superoxide dismutase enzyme (SOD), which allows the conversion of the highly reactive ROS, anion superoxide ($O_2^{\cdot-}$), in the less reactive one, hydrogen peroxide (H_2O_2) (Gonçalves et al., 2022; Guo et al., 2021). Moreover, SOD activity was also seen to be strictly correlated to catalase (CAT) enzymatic activity that, in fact, can finally convert H_2O_2 in water (H_2O), preventing ROS from binding to other molecules (Guo et al., 2021). Alteration of both SOD and CAT catalytic action was assessed in bivalves exposed to both MPs and NPs particles of different sizes and polymers, inducing changes in total oxidant status (TOS) and total antioxidant capacity (Sendra et al., 2021). For example, Gonçalves et al. (2022) found significant inhibition of SOD and CAT for *Mytilus galloprovincialis* specimens exposed for 21 days to nPS (50 nm). Time-dependent and tissue-dependent responses were also observed, whereby the gills seem to be the most affected tissue in the short term (3 and 7 days) with significant inhibition of both enzymes, whilst DG effects were less severe and visible after a longer exposure time (14 and 21 days) (Gonçalves et al., 2022). Guo et al. (2021) provided evidence on how, in the freshwater clam *Corbicula fluminea*, a very high increase in SOD activity after NPs (80 nm) and MPs (6 μ m) exposure, caused an overproduction of H_2O_2 , therefore overwhelming CAT enzyme, that is indeed inhibited. This means that the organism was not capable of counteracting ROS production, thus leading to an increased level of membrane lipid peroxidation (LPO) that indirectly reflects cell damage (Guo et al., 2021).

Results obtained here also show a time and tissue-dependent oxidative stress, whereby an increased enzymatic activity (SOD and CAT) was observed at the end of the exposure time. The digestive gland appears to be the most impacted tissue (Fig. 3.7.1 A & B and Fig. 3.7.2 A & B). Different uptake, translocation, and elimination processes associated with different tissues could explain those differences (Sikdokur et al., 2020). Indeed, once plastic ingestion occurs through feeding strategies from the gills, they can be redirected to the digestive gland, where they accumulate due to the absence of enzymatic pathways that allow plastic breakdown (Faggio et al., 2018; Wright et al., 2013). Moreover, the digestive gland in bivalves is involved in important digestive, food transfer/assimilation, and detoxification functions, potentially increasing its direct level of exposure to environmental pollutants and the overall effect on the organism (Détrée & Gallardo-Escárate, 2017; Guo et al., 2021). Ribeiro et al. (2017), for example, observed an important level of oxidative damage (increase LPO levels) in the digestive gland already after 7 days of exposure to *Scrobicularia plana* to PS MPs (18 μ m), whilst in gills lipid peroxidation was observed to decrease already after 3 days meaning a higher antioxidant system efficiency in this tissue (Li et al., 2019; Ribeiro et al., 2017). In both gills and digestive glands, the highest increase of enzyme catalytic activity is observed in relation to both mPE and Mix treatments (Fig. 3.7.1 A & B and Fig. 3.7.2 A & B). Nonetheless, also

nPS showed a time-dependent enzymatic induction that, although less important, affects only CAT in gills and SOD in the digestive gland (Fig. 3.7.1 A & B and Fig. 3.7.2 A & B).

Overall, the enzymatic antioxidant defense system of *R. decussatus* appears to be able to efficiently counteract plastic-induced ROS produced; thus, no signs of LPO are observed (Fig. 3.8.1 A and B). Moreover, a decrease in LPO was observed at day 10 in the gills of mPE-exposed organisms (Fig. 3.8.1 A). Ribeiro et al. (2017) also observed such an effect and might be related to the increased activity of antioxidant defenses. Indeed, as already mentioned before, in aerobic organisms, ROS are produced because of mitochondrial respiration (Bounous & Molson., 2003; Abele & Puntarulo, 2004), thus, even though their production is counteracted by the antioxidant defense system, a slight level of LPO can be present in unexposed clams. When environmental pollutants, as observed here, increase the activity of antioxidant enzymes, this might allow the organism to eliminate all oxygen reactive species more efficiently, thus causing a slight decrease of LPO in exposed organisms compared to controls.

Clam's hemocytes did not show any sign of DNA damage after 7 days of exposure for all treatments (Fig. 3.5.1 A and B). This might be related to the fact that, as mentioned before, once ingested, plastic particles are firstly translocated to the digestive gland, and only subsequently can they enter the circulatory system (Fossi et al., 2018; Sendra et al., 2021; Sikdokur et al., 2020; Wang et al., 2021). Thus, 7 days might not be a long enough time for the plastic particles to enter in contact with hemolymph cells inducing toxicity (Marisa et al., 2016). In accordance with the present results, Cole et al. (2020) also observed no DNA damage after exposing the mussel *M. edulis* to PS MPs (20 µm) for 7 days. Furthermore, Ribeiro et al. (2017) found no signs of an increase in % DNA tail in the clam *S. plana* after 14 days of exposure to PS MPs (18 µm). An increase was although observed after 7 days of post-exposure depuration, meaning that accumulated MPs that could not be egested had a delayed effect on DNA (Ribeiro et al., 2017). Genotoxicity could either be promoted directly by plastics-DNA interactions within the nucleus or indirectly through reactive oxygen species (ROS) production (Auguste et al., 2020; Marisa et al., 2016; Ribeiro et al., 2017). Therefore, the absence of effects could also be related to the efficient removal of ROS by the antioxidant system of the organism, as observed here in relation also to LPO (Fig. 3.8.1 A and B). Also, no signs of AChE inhibition were seen in the gills of *R. decussatus* exposed for 10 days to the different treatments (Fig. 3.6.1), indicating that no neurotoxicity occurred (Capolupo et al., 2021). However, an increase in its enzymatic activity was observed for specimens exposed to mPE and Mix treatments (Fig. 3.6.1). AChE plays an important role in voluntary muscle movement by catalyzing the breakdown of acetylcholine (ACh) after its interaction with neuromuscular synapsis for signal transmission (Guo et al., 2021). This allows to prevent continuous and uncontrolled muscular contractions (Guo et al.,

2021). Thus, an increase in its activity when organisms were exposed to bigger particles, as observed here (Fig. 3.6.1), might be related to the need for increasing muscular movement of gills filaments to avoid their constraint (Ward et al., 2019). Consequently, higher production of acetylcholine (ACh) is needed, potentially increasing AChE enzymatic activity for its degradation. This is in accordance with previously presented ingestion results, as the higher gills' capture efficiency for bigger aggregates might allow them to accumulate here before ingestion (Rosa et al., 2018; Ward et al., 2019).

Final biomarker data elaboration using a Principal Component Analysis (PCA) and the Weight of Evidence (WOE) quantitative model is in accordance with the observed time-specific responses for all tissues and treatments considered (Fig. 3.9.1 A & B and Fig. 3.11.1). MPs and NPs can induce intracellular ROS production due to their ability to enter inside cells (Hu & Palić, 2020). This process is regulated either by endocytosis (MPs) or pinocytosis (NPs), where particles incorporated in vesicles are brought inside the cells (Hu & Palić, 2020). Here they are treated as foreign material, thus triggering the innate immune system of the organism that, consequently, increases ROS production to neutralize possible damaging effects (Hu & Palić, 2020). Considering this, we can understand how a time lag between particle ingestion and the set-off of an effect might need to be considered. Moreover, it is also important to consider tissue translocation, which indeed might induce tissue and time-dependent effects (Capolupo et al., 2021; Gonçalves et al., 2022; Marisa et al., 2016).

This work contributes to a further understanding of how MPs and NPs behave in water and how their change in size can influence ingestion and toxic effects. Recent studies demonstrate how NPs, due to their smaller size, can more easily cross biological barriers and potentially interfere with important processes at molecular and cellular levels, likely in the long term (Capolupo et al., 2021; Gonçalves et al., 2023; Gonçalves et al., 2022; Gonçalves & Bebianno, 2021). MPs and NPs' tendency to form aggregates once dispersed in seawater (Li et al., 2019; Sun et al., 2021) is considered to increase their sizes, thus reducing the level of danger (Alimi et al., 2018; Gonçalves & Bebianno, 2021). This study assessed, for the first time, how MPs and NPs, when suspended together, tend to increase their level of aggregation (Fig. 3.1.2 and Fig. 3.1.4). This might also induce bigger changes in surface charge properties that, as previously mentioned, can be strictly related to organisms' selective feeding strategies. Moreover, both PCA and WOE results show that the most influential treatments on biomarker responses are mPE and Mix compared to nPS (Fig. 3.9.1 A & B and Fig. 3.11.1). Analyses of synergisms and antagonisms were also conducted to further understand how the interaction between MPs and NPs might pose a bigger threat to organisms (Table 3, 4, 5 and 6). In this case, a tissue-specific effect was observed, whereby in gills, a synergistic effect was observed for CAT (Table 5), which according to PCA and WOE, is one of the most influential biomarkers on the overall

effect (Fig. 3.9.1 A & B and Fig. 3.11.1). This is potentially related to the fact that gills capture efficiency asymptotically increases in relation to bigger aggregates (Ward et al., 2019) thus allowing them to be the first ones to enter in touch with them. On the other hand, antagonistic effects were observed in the digestive gland (Tables 4 and 6), where probably the biggest aggregates formed might be selectively egested either through pseudofeces or fecal pellets production (Ward et al., 2019). Different ingestion processes might occur depending on the particle sizes; indeed, NPs can be ingested through body adhesion and subsequential internal translocation (Gonçalves., 2023), while bigger particles are most likely captured by gills, ingested, and transported to the digestive gland (Fossi et al., 2018; Sendra et al., 2021; Sıkdokur et al., 2020; Wang et al., 2021; Ward et al., 2019). Thus, higher effects observed here in relation to bigger particles might be because particles ingested through water filtration potentially enter faster in touch with gills and digestive glands. Therefore, a longer time of exposure is needed to better comprehend alteration in the long term, especially in relation to nPS. In accordance with this, this work shows a higher level of toxicity when cells were exposed *in vitro* to nPS. As mentioned before, this possibly means that nPS's smaller size can induce more severe effects at the cellular level (Gonçalves & Bebianno, 2021). Nonetheless, this study clearly shows the possibility of bigger particles to induce intracellular alterations potentially more rapidly due to their higher capture efficiency also correlated to important levels of ingestion. Even though no effective signs of oxidative damage were observed, a possible co-exposure of organisms to smaller and bigger plastics fragments, an environmentally realistic condition, might induce a longer stimulation of the antioxidant defense system reducing the amount of energy available for important biological processes such as growth and reproduction (Trestrall et al., 2020). Furthermore, the formation of bigger aggregates because of higher combining potential, can also induce important post-ingestion mechanical damage (Fossi et al., 2018; Capolupo et al., 2021; Teng et al., 2021). Therefore, in future studies, it would be also useful to assess particles rejection mechanisms to better define particle size limits related to bivalves' ingestion.

CONCLUSION

This dataset provides evidence of the interaction of two different polymers (PS and PE) of plastic at different sizes (MPs and NPs) and their toxicity towards the clam *R. decussatus*. Ingestion of these particles was seen to be independent of the particle size as nPS, mPE, and the bigger aggregates formed when in a mixture with each other are highly ingested by the clam. Individual NPs induced important effects on cellular viability and time and tissue-dependent oxidative stress. Nonetheless, mPE and Mix's treatments were seen to be the most influential treatments causing essential changes in the short term in the antioxidant enzymes' (SOD, CAT) activity. Moreover, no signs of oxidative

damage, genotoxicity, and neurotoxicity were seen for all treatments in the short term. Antagonistic interactions in gills and antagonistic ones in the digestive gland between MPs and NPs were observed here. However, a longer exposure time and particles' egestion mechanisms should be further evaluated to better understand results. Furthermore, there is also the need to assess the ability of MPs and NPs of the same polymer to form aggregates and evaluate the level of toxicity of other polymers that may be found in the environment (e.g., PET, PP, PVC).

BIBLIOGRAPHY

24-The-Antioxidant-System. 2003.

Abdul Rahman, A. M. N. A., Yan, L. Z., Abdul Hamid, Z. A., Ku Ishak, K. M., Abdullah, M. K., Rusli, A., Khimi Shuib, R., Mohd Zaini Makthar, M., & Shafiq, M. D. (2023). Surface interactions of model microplastic particles in seawater. *Progress in Rubber, Plastics and Recycling Technology*, 39(1), 3–11. <https://doi.org/10.1177/14777606221128043>

Abele, D., & Puntarulo, S. (2004). Formation of reactive species and induction of antioxidant defence systems in polar and temperate marine invertebrates and fish. In *Comparative Biochemistry and Physiology - A Molecular and Integrative Physiology* (Vol. 138, Issue 4, pp. 405–415). Elsevier Inc. <https://doi.org/10.1016/j.cbpb.2004.05.013>

Abidli, S., Lahbib, Y., & Trigui El Menif, N. (2019). Microplastics in commercial molluscs from the lagoon of Bizerte (Northern Tunisia). *Marine Pollution Bulletin*, 142, 243–252. <https://doi.org/10.1016/j.marpolbul.2019.03.048>

Alimi, O. S., Farner Budarz, J., Hernandez, L. M., & Tufenkji, N. (2018). Microplastics and Nanoplastics in Aquatic Environments: Aggregation, Deposition, and Enhanced Contaminant Transport. In *Environmental Science and Technology* (Vol. 52, Issue 4, pp. 1704–1724). American Chemical Society. <https://doi.org/10.1021/acs.est.7b05559>

Anhichem, M., Yahyaoui, A., Adil, O., Bessa, A., & Benbrahim, S. (2021). Evaluation of the growth potential and contamination of the European clam (*Ruditapes decussatus*) raised using the suspension culture technique at the Oualidia lagoon in (Vol. 14, Issue 2). <http://www.bioflux.com.ro/aac1>

Aníbal, J., Gomes, A., Mendes, I., & Moura, D. (n.d.). Challenges of a coastal lagoon in a changing environment CIMA CENTRO DE INVESTIGAÇÃO MARINHA E AMBIENTAL.

Auguste, M., Lasa, A., Balbi, T., Pallavicini, A., Vezzulli, L., & Canesi, L. (2020). Impact of nanoplastics on hemolymph immune parameters and microbiota composition in *Mytilus galloprovincialis*. *Marine Environmental Research*, 159. <https://doi.org/10.1016/j.marenvres.2020.105017>

Barboza, L. G. A., Vieira, L. R., & Guilhermino, L. (2018). Single and combined effects of microplastics and mercury on juveniles of the European seabass (*Dicentrarchus labrax*): Changes in behavioural responses and reduction of swimming velocity and resistance time. *Environmental Pollution*, 236, 1014–1019. <https://doi.org/10.1016/j.envpol.2017.12.082>

Baudrimont, M., Arini, A., Guégan, C., Venel, Z., Gigault, J., Pedrono, B., Prunier, J., Maurice, L., Ter Halle, A., & Feurtet-Mazel, A. (2020). Ecotoxicity of polyethylene nanoplastics from the North Atlantic oceanic gyre on freshwater and marine organisms (microalgae and filter-feeding

- bivalves). *Environmental Science and Pollution Research*, 27(4), 3746–3755. <https://doi.org/10.1007/s11356-019-04668-3>
- Bebianno, M. J., G eret, F., Hoarau, P., Serafim, M. A., Coelho, M. R., Gnassia-Barelli, M., & Rom eo, M. (2004). Biomarkers in *Ruditapes decussatus*: A potential bioindicator species. In *Biomarkers* (Vol. 9, Issues 4–5, pp. 305–330). <https://doi.org/10.1080/13547500400017820>
- Bendell, L. I., LeCadre, E., & Zhou, W. (2020). Use of sediment dwelling bivalves to biomonitor plastic particle pollution in intertidal regions; A review and study. *PLoS ONE*, 15(5). <https://doi.org/10.1371/journal.pone.0232879>
- Benedetti, M., Giuliani, M. E., Mezzelani, M., Nardi, A., Pittura, L., Gorbi, S., & Regoli, F. (2022). Emerging environmental stressors and oxidative pathways in marine organisms: Current knowledge on regulation mechanisms and functional effects. In *Biocell* (Vol. 46, Issue 1, pp. 37–49). Tech Science Press. <https://doi.org/10.32604/biocell.2022.017507>
- Bergami, E., Krupinski Emerenciano, A., Gonz alez-Aravena, M., C ardenas, C. A., Hern andez, P., Silva, J. R. M. C., & Corsi, I. (2019). Polystyrene nanoparticles affect the innate immune system of the Antarctic sea urchin *Sterechinus neumayeri*. *Polar Biology*, 42(4), 743–757. <https://doi.org/10.1007/s00300-019-02468-6>
- Bradford, M. M. (1976). A Rapid and Sensitive Method for the Quantitation of Microgram Quantities of Protein Utilizing the Principle of Protein-Dye Binding. In *ANALYTICAL BIOCHEMISTRY* (Vol. 72).
- Brandts, I., Barr a, C., Martins, M. A., Franco-Mart inez, L., Barreto, A., Tvarijonaviciute, A., Tort, L., Oliveira, M., & Teles, M. (2021). Waterborne exposure of gilthead seabream (*Sparus aurata*) to polymethylmethacrylate nanoplastics causes effects at cellular and molecular levels. *Journal of Hazardous Materials*, 403. <https://doi.org/10.1016/j.jhazmat.2020.123590>
- Brandts, I., Teles, M., Tvarijonaviciute, A., Pereira, M. L., Martins, M. A., Tort, L., & Oliveira, M. (2018). Effects of polymethylmethacrylate nanoplastics on *Dicentrarchus labrax*. *Genomics*, 110(6), 435–441. <https://doi.org/10.1016/j.ygeno.2018.10.006>
- Browne, M. A., Dissanayake, A., Galloway, T. S., Lowe, D. M., & Thompson, R. C. (2008). Ingested microscopic plastic translocate to the circulatory system of the mussel, *Mytilus edulis* (L.). *Environmental Science and Technology*, 42(13), 5026–5031. <https://doi.org/10.1021/es800249a>
- Capolupo, M., Valbonesi, P., & Fabbri, E. (2021). A comparative assessment of the chronic effects of micro-and nano-plastics on the physiology of the Mediterranean mussel *Mytilus galloprovincialis*. *Nanomaterials*, 11(3), 1–17. <https://doi.org/10.3390/nano11030649>

- Cole, M., Liddle, C., Consolandi, G., Drago, C., Hird, C., Lindeque, P. K., & Galloway, T. S. (2020). Microplastics, microfibers and nanoplastics cause variable sub-lethal responses in mussels (*Mytilus spp.*). *Marine Pollution Bulletin*, 160. <https://doi.org/10.1016/j.marpolbul.2020.111552>
- Cozzolino, L., De Los Santos, C. B., Zardi, G. I., Repetto, L., & Nicastro, K. R. (2021). Microplastics in commercial bivalves harvested from intertidal seagrasses and sandbanks in the Ria Formosa lagoon, Portugal. *Marine and Freshwater Research*, 72(7), 1092–1099. <https://doi.org/10.1071/MF20202>
- de Alkimin, G. D., Gonçalves, J. M., Nathan, J., & Bebianno, M. J. (2022). Impact of micro and nanoplastics in the marine environment. In *Assessing the Effects of Emerging Plastics on the Environment and Public Health* (pp. 172–225). IGI Global. <https://doi.org/10.4018/978-1-7998-9723-1.ch009>
- Détrée, C., & Gallardo-Escárate, C. (2017). Polyethylene microbeads induce transcriptional responses with tissue-dependent patterns in the mussel *Mytilus galloprovincialis*. *Journal of Molluscan Studies*, 83(2), 220–225. <https://doi.org/10.1093/mollus/eyx005>
- Dias De Alkimin, G., Gonçalves, J. M., Nathan, J., & Bebianno, M. J. (n.d.). Impact of micro-and nanoplastics in the marine environment.
- Duis, K., & Coors, A. (2016). Microplastics in the aquatic and terrestrial environment: sources (with a specific focus on personal care products), fate and effects. In *Environmental Sciences Europe* (Vol. 28, Issue 1, pp. 1–25). Springer Verlag. <https://doi.org/10.1186/s12302-015-0069-y>
- Ekvall, M. T., Lundqvist, M., Kelpsiene, E., Šileikis, E., Gunnarsson, S. B., & Cedervall, T. (2019). Nanoplastics formed during the mechanical breakdown of daily-use polystyrene products. *Nanoscale Advances*, 1(3), 1055–1061. <https://doi.org/10.1039/c8na00210j>
- Ellman, G. L., Courtney, K. D., Andres, V., & Featherstone, R. M. (1961). A NEW AND RAPID COLORIMETRIC DETERMINATION OF ACETYLCHOLINESTERASE ACTIVITY. In *Biochemical Pharmacology* (Vol. 7). Pergamon Press Ltd.
- El-Sherif, D. M., Eloffy, M. G., Elmesery, A., Abouzid, M., Gad, M., El-Seedi, H. R., Brinkmann, M., Wang, K., & Al Naggar, Y. (2022). Environmental risk, toxicity, and biodegradation of polyethylene: a review. In *Environmental Science and Pollution Research* (Vol. 29, Issue 54, pp. 81166–81182). Springer Science and Business Media Deutschland GmbH. <https://doi.org/10.1007/s11356-022-23382-1>
- Erdelmeier, I., Gérard-Monnier, D., Yadan, J. C., & Chaudière, J. (1998). Reactions of N-methyl-2-phenylindole with malondialdehyde and 4- hydroxyalkenals. Mechanistic aspects of the colorimetric assay of lipid peroxidation. *Chemical Research in Toxicology*, 11(10), 1184–1194. <https://doi.org/10.1021/tx970180z>

- Espinosa, C., García Beltrán, J. M., Esteban, M. A., & Cuesta, A. (2018). In vitro effects of virgin microplastics on fish head-kidney leucocyte activities. *Environmental Pollution*, 235, 30–38. <https://doi.org/10.1016/j.envpol.2017.12.054>
- Faggio, C., Tsarpali, V., & Dailianis, S. (2018). Mussel digestive gland as a model tissue for assessing xenobiotics: An overview. In *Science of the Total Environment* (Vol. 636, pp. 220–229). Elsevier B.V. <https://doi.org/10.1016/j.scitotenv.2018.04.264>
- FAO - microplastic in fisheries. (2017).
- Fossi, M. C., Pedà, C., Compa, M., Tsangaris, C., Alomar, C., Claro, F., Ioakeimidis, C., Galgani, F., Hema, T., Deudero, S., Romeo, T., Battaglia, P., Andaloro, F., Caliani, I., Casini, S., Panti, C., & Baini, M. (2018). Bioindicators for monitoring marine litter ingestion and its impacts on Mediterranean biodiversity. In *Environmental Pollution* (Vol. 237, pp. 1023–1040). Elsevier Ltd. <https://doi.org/10.1016/j.envpol.2017.11.019>
- Gagné, F. (2019). Detection of polystyrene nanoplastics in biological tissues with a fluorescent molecular rotor probe. *Journal of Xenobiotics*. <https://doi.org/10.4081/xeno.2019.8147>
- Gambardella, C., Morgana, S., Ferrando, S., Bramini, M., Piazza, V., Costa, E., Garaventa, F., & Faimali, M. (2017). Effects of polystyrene microbeads in marine planktonic crustaceans. *Ecotoxicology and Environmental Safety*, 145, 250–257. <https://doi.org/10.1016/j.ecoenv.2017.07.036>
- Gaspar, T. R., Chi, R. J., Parrow, M. W., & Ringwood, A. H. (2018). Cellular bioreactivity of micro- and nano-plastic particles in oysters. *Frontiers in Marine Science*, 5(OCT). <https://doi.org/10.3389/fmars.2018.00345>
- Gigault, J., Halle, A. ter, Baudrimont, M., Pascal, P. Y., Gauffre, F., Phi, T. L., El Hadri, H., Grassl, B., & Reynaud, S. (2018). Current opinion: What is a nanoplastic? In *Environmental Pollution* (Vol. 235, pp. 1030–1034). Elsevier Ltd. <https://doi.org/10.1016/j.envpol.2018.01.024>
- Gomes, T., Almeida, A. C., & Georgantzopoulou, A. (2020). Characterization of cell responses in *Rhodomonas baltica* exposed to PMMA nanoplastics. *Science of the Total Environment*, 726. <https://doi.org/10.1016/j.scitotenv.2020.138547>
- Gomes, T., Araújo, O., Pereira, R., Almeida, A. C., Cravo, A., & Bebianno, M. J. (2013). Genotoxicity of copper oxide and silver nanoparticles in the mussel *Mytilus galloprovincialis*. *Marine Environmental Research*, 84, 51–59. <https://doi.org/10.1016/j.marenvres.2012.11.009>
- Gómez-Mendikute, A., & Cajaraville, M. P. (2003). Comparative effects of cadmium, copper, paraquat and benzo[a]pyrene on the actin cytoskeleton and production of reactive oxygen species (ROS) in mussel haemocytes. *Toxicology in Vitro*, 17(5–6), 539–546. [https://doi.org/10.1016/S0887-2333\(03\)00093-6](https://doi.org/10.1016/S0887-2333(03)00093-6)

- Gonçalves, J. M., & Bebianno, M. J. (2021). Nanoplastics impact on marine biota: A review. *Environmental Pollution*, 273. <https://doi.org/10.1016/j.envpol.2021.116426>
- Gonçalves, J. M., Sousa, V. S., Teixeira, M. R., & Bebianno, M. J. (2022). Chronic toxicity of polystyrene nanoparticles in the marine mussel *Mytilus galloprovincialis*. *Chemosphere*, 287. <https://doi.org/10.1016/j.chemosphere.2021.132356>
- Gonçalves, J. M., Benedetti Giuseppe D'errico, M., Regoli, F., Bebianno, M. J., Gagné, F., Canesi, L., & Galloway, T. (2023). Environmental Pollution Polystyrene nanoplastics in the marine mussel *Mytilus galloprovincialis*. Powered by Editorial Manager® and ProduXion Manager® from Aries Systems Corporation.
- Guo, X., Cai, Y., Ma, C., Han, L., & Yang, Z. (2021). Combined toxicity of micro/nano scale polystyrene plastics and ciprofloxacin to *Corbicula fluminea* in freshwater sediments. *Science of the Total Environment*, 789. <https://doi.org/10.1016/j.scitotenv.2021.147887>
- Guzzetti, E., Sureda, A., Tejada, S., & Faggio, C. (2018). Microplastic in marine organism: Environmental and toxicological effects. In *Environmental Toxicology and Pharmacology* (Vol. 64, pp. 164–171). Elsevier B.V. <https://doi.org/10.1016/j.etap.2018.10.009>
- Horn, D. A., Granek, E. F., & Steele, C. L. (2020). Effects of environmentally relevant concentrations of microplastic fibers on Pacific mole crab (*Emerita analoga*) mortality and reproduction. In *Limnology And Oceanography Letters* (Vol. 5, Issue 1, pp. 74–83). John Wiley and Sons Inc. <https://doi.org/10.1002/lo2.10137>
- Hsieh, S.-L., Hsieh, S., Xu, R.-Q., Chen, Y.-T., Chen, C.-W., Singhanian, R. R., Chen, Y.-C., Tsai, T.-H., & Dong, C.-D. (2023). Toxicological effects of polystyrene nanoplastics on marine organisms. *Environmental Technology & Innovation*, 30, 103073. <https://doi.org/10.1016/j.eti.2023.103073>
- Hu, M., & Palić, D. (2020). Micro- and nano-plastics activation of oxidative and inflammatory adverse outcome pathways. In *Redox Biology* (Vol. 37). Elsevier B.V. <https://doi.org/10.1016/j.redox.2020.101620>
- Huang, W., Wang, X., Chen, D., Xu, E. G., Luo, X., Zeng, J., Huan, T., Li, L., & Wang, Y. (2021). Toxicity mechanisms of polystyrene microplastics in marine mussels revealed by high-coverage quantitative metabolomics using chemical isotope labeling liquid chromatography mass spectrometry. *Journal of Hazardous Materials*, 417. <https://doi.org/10.1016/j.jhazmat.2021.126003>
- Islam, N., Garcia da Fonseca, T., Vilke, J., Gonçalves, J. M., Pedro, P., Keiter, S., Cunha, S. C., Fernandes, J. O., & Bebianno, M. J. (2021). Perfluorooctane sulfonic acid (PFOS) adsorbed to polyethylene microplastics: Accumulation and ecotoxicological effects in the clam

Scrobicularia plana. Marine Environmental Research, 164.

<https://doi.org/10.1016/j.marenvres.2020.105249>

- Jambeck, J. R., Geyer, R., Wilcox, C., Siegler, T. R., Perryman, M., Andrady, A., Narayan, R., & Law, K. L. (2015). Plastic waste inputs from land into the ocean. *Science*, 347(6223), 768–771. <https://doi.org/10.1126/science.1260352>
- João Da Anunciação, M., Bebianno, F., & Nathan, J. E. (2022). Presence of microplastic in commercial bivalves along the Portuguese coast, comparing different aquaculture systems. Mestrado em Biologia Marinha Supervisor: Co-supervisor.
- Katsumiti, A., Gilliland, D., Arostegui, I., & Cajaraville, M. P. (2014). Cytotoxicity and cellular mechanisms involved in the toxicity of CdS quantum dots in hemocytes and gill cells of the mussel *Mytilus galloprovincialis*. *Aquatic Toxicology*, 153, 39–52. <https://doi.org/10.1016/j.aquatox.2014.02.003>
- Kiran, B. R., Kopperi, H., & Venkata Mohan, S. (2022). Micro/nano-plastics occurrence, identification, risk analysis and mitigation: challenges and perspectives. In *Reviews in Environmental Science and Biotechnology* (Vol. 21, Issue 1, pp. 169–203). Springer Science and Business Media B.V. <https://doi.org/10.1007/s11157-021-09609-6>
- Lee, K. W., Shim, W. J., Kwon, O. Y., & Kang, J. H. (2013). Size-dependent effects of micro polystyrene particles in the marine copepod *Tigriopus japonicus*. *Environmental Science and Technology*, 47(19), 11278–11283. <https://doi.org/10.1021/es401932b>
- Lei, L., Wu, S., Lu, S., Liu, M., Song, Y., Fu, Z., Shi, H., Raley-Susman, K. M., & He, D. (2018). Microplastic particles cause intestinal damage and other adverse effects in zebrafish *Danio rerio* and nematode *Caenorhabditis elegans*. *Science of the Total Environment*, 619–620, 1–8. <https://doi.org/10.1016/j.scitotenv.2017.11.103>
- Li, Y., Wang, X., Fu, W., Xia, X., Liu, C., Min, J., Zhang, W., & Crittenden, J. C. (2019). Interactions between nano/micro plastics and suspended sediment in water: Implications on aggregation and settling. *Water Research*, 161, 486–495. <https://doi.org/10.1016/j.watres.2019.06.018>
- Manfra, L., Rotini, A., Bergami, E., Grassi, G., Faleri, C., & Corsi, I. (2017). Comparative ecotoxicity of polystyrene nanoparticles in natural seawater and reconstituted seawater using the rotifer *Brachionus plicatilis*. *Ecotoxicology and Environmental Safety*, 145, 557–563. <https://doi.org/10.1016/j.ecoenv.2017.07.068>
- Marisa, I., Matozzo, V., Munari, M., Binelli, A., Parolini, M., Martucci, A., Franceschinis, E., Brianese, N., & Marin, M. G. (2016). In vivo exposure of the marine clam *Ruditapes philippinarum* to zinc oxide nanoparticles: responses in gills, digestive gland and haemolymph.

- Environmental Science and Pollution Research, 23(15), 15275–15293.
<https://doi.org/10.1007/s11356-016-6690-5>
- Mccords, J. M., & Fridovich, I. (1969). Superoxide Dismutase AN ENZYMIC FUNCTION FOR ERYTHROCUPREIN (HEMOCUPREIN)*. In THE JOURNAL OF BIOLOGICAL CHEMISTRY (Vol. 244, Issue 22).
- Mohsen, M., Sun, L., Lin, C., Huo, D., & Yang, H. (2021). Mechanism underlying the toxicity of the microplastic fibre transfer in the sea cucumber *Apostichopus japonicus*. Journal of Hazardous Materials, 416. <https://doi.org/10.1016/j.jhazmat.2021.125858>
- Ning, Q., Wang, D., An, J., Ding, Q., Huang, Z., Zou, Y., Wu, F., & You, J. (2022). Combined effects of nanosized polystyrene and erythromycin on bacterial growth and resistance mutations in *Escherichia coli*. Journal of Hazardous Materials, 422. <https://doi.org/10.1016/j.jhazmat.2021.126858>
- Plastics the facts (2022).
- Pirsaheb, M., Hossini, H., & Makhdoumi, P. (2020). Review of microplastic occurrence and toxicological effects in marine environment: Experimental evidence of inflammation. In Process Safety and Environmental Protection (Vol. 142, pp. 1–14). Institution of Chemical Engineers. <https://doi.org/10.1016/j.psep.2020.05.050>
- PlasticsEurope. (2021). Plastics-the Facts 2021 An analysis of European plastics production, demand and waste data.
- Ramaswamy, V., & Rao, P. S. (2006). Grain size analysis of sediments from the northern Andaman Sea: Comparison of laser diffraction and sieve-pipette techniques. Journal of Coastal Research, 22(4), 1000–1009. <https://doi.org/10.2112/04-0162.1>
- Regoli, F., d’Errico, G., Nardi, A., Mezzelani, M., Fattorini, D., Benedetti, M., Di Carlo, M., Pellegrini, D., & Gorbi, S. (2019). Application of a weight of evidence approach for monitoring complex environmental scenarios: The case-study of off-shore platforms. Frontiers in Marine Science, 6(JUL). <https://doi.org/10.3389/fmars.2019.00377>
- Repetto, G., del Peso, A., & Zurita, J. L. (2008). Neutral red uptake assay for the estimation of cell viability/ cytotoxicity. Nature Protocols, 3(7), 1125–1131. <https://doi.org/10.1038/nprot.2008.75>
- Ribeiro, F., Garcia, A. R., Pereira, B. P., Fonseca, M., Mestre, N. C., Fonseca, T. G., Ilharco, L. M., & Bebianno, M. J. (2017). Microplastics effects in *Scrobicularia plana*. Marine Pollution Bulletin, 122(1–2), 379–391. <https://doi.org/10.1016/j.marpolbul.2017.06.078>

- Ritz, C., Streibig, J. C., & Kniss, A. (2021). How to use statistics to claim antagonism and synergism from binary mixture experiments. In *Pest Management Science* (Vol. 77, Issue 9, pp. 3890–3899). John Wiley and Sons Ltd. <https://doi.org/10.1002/ps.6348>
- Rodrigues, A. R., Mestre, N. C. C., da Fonseca, T. G., Pedro, P. Z., Carteny, C. C., Cormier, B., Keiter, S., & Bebianno, M. J. (2022). Influence of Particle Size on Ecotoxicity of Low-Density Polyethylene Microplastics, with and without Adsorbed Benzo-a-Pyrene, in Clam *Scrobicularia plana*. *Biomolecules*, 12(1). <https://doi.org/10.3390/biom12010078>
- Rodríguez, J. G., & Uriarte, A. (2009). Laser diffraction and dry-sieving grain size analyses undertaken on fine- and medium-grained sandy marine sediments: A note. *Journal of Coastal Research*, 25(1), 257–264. <https://doi.org/10.2112/08-1012.1>
- Rosa, M., Evan Ward, J., Shumwy, S. E., & Evan, J. (2018). Selective capture and ingestion of particles by suspension-Selective capture and ingestion of particles by suspension-feeding bivalve molluscs: a review <https://digitalcommons.conncoll.edu/biofacpub/37>
- Rosa, M., Ward, J. E., Frink, A., & Shumway, S. E. (2017). Effects of Surface Properties on Particle Capture by Two Species of Suspension-Feeding Bivalve Molluscs. *American Malacological Bulletin*, 35(2), 181–188. <https://doi.org/10.4003/006.035.0212>
- Sendra, M., Sparaventi, E., Novoa, B., & Figueras, A. (2021). An overview of the internalization and effects of microplastics and nanoplastics as pollutants of emerging concern in bivalves. In *Science of the Total Environment* (Vol. 753). Elsevier B.V. <https://doi.org/10.1016/j.scitotenv.2020.142024>
- Shams, M., Alam, I., & Chowdhury, I. (2020). Aggregation and stability of nanoscale plastics in aquatic environment. *Water Research*, 171. <https://doi.org/10.1016/j.watres.2019.115401>
- Silva, S., Cravo, A., Ferreira, C., Correia, C., & Almeida, C. M. M. (2021). Biomarker Responses of the Clam *Ruditapes decussatus* Exposed to a Complex Mixture of Environmental Stressors under the Influence of an Urban Wastewater-Treatment Plant. *Environmental Toxicology and Chemistry*, 40(1), 272–283. <https://doi.org/10.1002/etc.4895>
- Singh, N. P., McCoy, M. T., Tice, R. R., & Schneider, E. L. (1988). A Simple Technique for Quantitation of Low Levels of DNA Damage in Individual Cells'. In *Experimental Cell Research* (Vol. 175).
- Sikdokur, E., Belivermiş, M., Sezer, N., Pekmez, M., Bulan, Ö. K., & Kılıç, Ö. (2020). Effects of microplastics and mercury on manila clam *Ruditapes philippinarum*: Feeding rate, immunomodulation, histopathology, and oxidative stress. *Environmental Pollution*, 262. <https://doi.org/10.1016/j.envpol.2020.114247>

- Sobral, P., & Widdows, J. (2000). Effects of increasing current velocity, turbidity and particle-size selection on the feeding activity and scope for growth of *Ruditapes decussatus* from Ria Formosa, southern Portugal. In *Journal of Experimental Marine Biology and Ecology* (Vol. 245). www.elsevier.nl/locate/jembe
- Sun, H., Jiao, R., & Wang, D. (2021). The difference of aggregation mechanism between microplastics and nanoplastics: Role of Brownian motion and structural layer force. *Environmental Pollution*, 268. <https://doi.org/10.1016/j.envpol.2020.115942>
- Sun, X., Chen, B., Li, Q., Liu, N., Xia, B., Zhu, L., & Qu, K. (2018). Toxicities of polystyrene nano- and microplastics toward marine bacterium *Halomonas alkaliphila*. *Science of the Total Environment*, 642, 1378–1385. <https://doi.org/10.1016/j.scitotenv.2018.06.141>
- Ter Halle, A., Jeanneau, L., Martignac, M., Jardé, E., Pedrono, B., Brach, L., & Gigault, J. (2017). Nanoplastic in the North Atlantic Subtropical Gyre. *Environmental Science and Technology*, 51(23), 13689–13697. <https://doi.org/10.1021/acs.est.7b03667>
- Thomas, M., Jon, B., Craig, S., Edward, R., Ruth, H., John, B., Dick, V. A., Heather, L. A., & Matthew, S. (2020). The world is your oyster: low-dose, long-term microplastic exposure of juvenile oysters. *Heliyon*, 6(1). <https://doi.org/10.1016/j.heliyon.2019.e03103>
- Thushari, G. G. N., & Senevirathna, J. D. M. (2020). Plastic pollution in the marine environment. In *Heliyon* (Vol. 6, Issue 8). Elsevier Ltd. <https://doi.org/10.1016/j.heliyon.2020.e04709>
- Ustabasi, G. S., & Baysal, A. (2020). Bacterial interactions of microplastics extracted from toothpaste under controlled conditions and the influence of seawater. *Science of the Total Environment*, 703. <https://doi.org/10.1016/j.scitotenv.2019.135024>
- Van Cauwenberghe, L., Devriese, L., Galgani, F., Robbins, J., & Janssen, C. R. (2015). Microplastics in sediments: A review of techniques, occurrence, and effects. *Marine Environmental Research*, 111, 5–17. <https://doi.org/10.1016/j.marenvres.2015.06.007>
- Venâncio, C., Ferreira, I., Martins, M. A., Soares, A. M. V. M., Lopes, I., & Oliveira, M. (2019). The effects of nanoplastics on marine plankton: A case study with polymethylmethacrylate. *Ecotoxicology and Environmental Safety*, 184. <https://doi.org/10.1016/j.ecoenv.2019.109632>
- Vital, S. A., Cardoso, C., Avio, C., Pittura, L., Regoli, F., & Bebianno, M. J. (2021). Do microplastic contaminated seafood consumption pose a potential risk to human health? *Marine Pollution Bulletin*, 171. <https://doi.org/10.1016/j.marpolbul.2021.112769>
- Wang, S., Hu, M., Zheng, J., Huang, W., Shang, Y., Kar-Hei Fang, J., Shi, H., & Wang, Y. (2021). Ingestion of nano/micro plastic particles by the mussel *Mytilus coruscus* is size dependent. *Chemosphere*, 263. <https://doi.org/10.1016/j.chemosphere.2020.127957>

- Ward, J. E., Rosa, M., & Shumway, S. E. (2019). Capture, ingestion, and egestion of microplastics by suspension-feeding bivalves: A 40-year history. *Anthropocene Coasts*, 2(1), 39–49. <https://doi.org/10.1139/anc-2018-0027>
- Ward, J. E., & Shumway, S. E. (2004). Separating the grain from the chaff: Particle selection in suspension- and deposit-feeding bivalves. *Journal of Experimental Marine Biology and Ecology*, 300(1–2), 83–130. <https://doi.org/10.1016/j.jembe.2004.03.002>
- Wright, S. L., Thompson, R. C., & Galloway, T. S. (2013). The physical impacts of microplastics on marine organisms: a review. In *Environmental pollution* (Barking, Essex : 1987) (Vol. 178, pp. 483–492). <https://doi.org/10.1016/j.envpol.2013.02.031>
- Zaki, M. R. M., & Aris, A. Z. (2022). An overview of the effects of nanoplastics on marine organisms. In *Science of the Total Environment* (Vol. 831). Elsevier B.V. <https://doi.org/10.1016/j.scitotenv.2022.154757>
- Zhang, K., Hamidian, A. H., Tubić, A., Zhang, Y., Fang, J. K. H., Wu, C., & Lam, P. K. S. (2021). Understanding plastic degradation and microplastic formation in the environment: A review. In *Environmental Pollution* (Vol. 274). Elsevier Ltd. <https://doi.org/10.1016/j.envpol.2021.116554>
- Zhou, Y., He, G., Jiang, H., Pan, K., & Liu, W. (2023). Nanoplastics induces oxidative stress and triggers lysosome-associated immune-defensive cell death in the earthworm *Eisenia fetida*. *Environment International*, 174. <https://doi.org/10.1016/j.envint.2023.107899>
- Ziccardi, L. M., Edgington, A., Hentz, K., Kulacki, K. J., & Kane Driscoll, S. (2016). Microplastics as vectors for bioaccumulation of hydrophobic organic chemicals in the marine environment: A state-of-the-science review. *Environmental Toxicology and Chemistry*, 35(7), 1667–1676. <https://doi.org/10.1002/etc.3461>